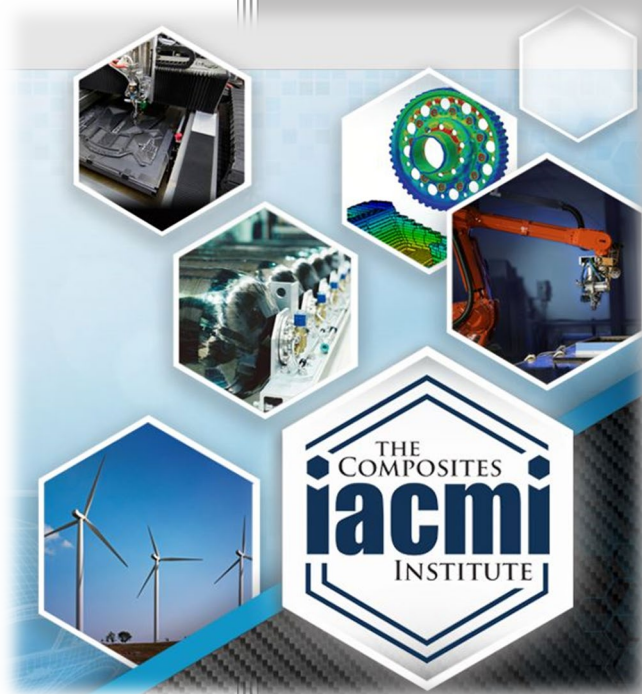


# Process and Applications Development for Recycled Mixed-Stream Composites



Author: Daniel Coughlin  
Date: March 23, 2022

**Final Technical Report  
PA16-0349-6.29-01**

**Approved for Public Release.  
Distribution is Unlimited.**



U.S. DEPARTMENT OF  
**ENERGY**

## DOCUMENT AVAILABILITY

Reports produced after January 1, 1996, are generally available free via US Department of Energy (DOE) SciTech Connect.

**Website** <http://www.osti.gov/scitech/>

Reports produced before January 1, 1996, may be purchased by members of the public from the following source:

National Technical Information Service  
5285 Port Royal Road  
Springfield, VA 22161  
**Telephone** 703-605-6000 (1-800-553-6847)  
**TDD** 703-487-4639  
**Fax** 703-605-6900  
**E-mail** [info@ntis.gov](mailto:info@ntis.gov)  
**Website** <http://www.ntis.gov/help/ordermethods.aspx>

Reports are available to DOE employees, DOE contractors, Energy Technology Data Exchange representatives, and International Nuclear Information System representatives from the following source:

Office of Scientific and Technical Information  
PO Box 62  
Oak Ridge, TN 37831  
**Telephone** 865-576-8401  
**Fax** 865-576-5728  
**E-mail** [reports@osti.gov](mailto:reports@osti.gov)  
**Website** <http://www.osti.gov/contact.html>

Disclaimer: "The information, data, or work presented herein was funded in part by an agency of the United States Government. Neither the United States Government nor any agency thereof, nor any of their employees, makes any warranty, express or implied, or assumes any legal liability or responsibility for the accuracy, completeness, or usefulness of any information, apparatus, product, or process disclosed, or represents that its use would not infringe privately owned rights. Reference herein to any specific commercial product, process, or service by trade name, trademark, manufacturer, or otherwise does not necessarily constitute or imply its endorsement, recommendation, or favoring by the United States Government or any agency thereof. The views and opinions of authors expressed herein do not necessarily state or reflect those of the United States Government or any agency thereof."

The information, data, or work presented herein was funded in part by the Office of Energy Efficiency and Renewable Energy (EERE), U.S. Department of Energy, under Award DE- EE0006926.

# Process and Applications Development for Recycled Mixed-Stream Composites

Principal Investigator: Daniel Coughlin

Organization: American Composites Manufacturers Association

Address: 2000 N. 15th Street, Ste. 250. Arlington, VA 22201

Phone: (703) 525-0743

Email: [dcoughlin@acmanet.org](mailto:dcoughlin@acmanet.org)

Co-authors: Ryan Ginder, University of Tennessee  
Michael Gruskiewicz, LyondellBassell  
David Hartman, Owens Corning  
Charles Ludwig, CHZ Technologies  
Soydan Ozcan, Oak Ridge National Laboratory  
David R. Salem, South Dakota School of Mines and Technology  
Paula Stevenson, UVG Group  
Halil Tekinalp, Oak Ridge National Laboratory  
Uday Vaidya, University of Tennessee  
N. Krishnan P. Veluswamy, South Dakota School of Mines and Technology  
Sanjita Wasti, Oak Ridge National Laboratory  
Xianhui Zhao, Oak Ridge National Laboratory

Date Published: (March, 2022)

Prepared by:  
Institute for Advanced Composites Manufacturing Innovation  
Knoxville, TN 37932  
Managed by Collaborative Composite Solutions, Inc.  
For the  
U.S. DEPARTMENT OF ENERGY  
Under contract DE- EE0006926

Project Period:  
(08/2019 – 12/2020)

## TABLE OF CONTENTS

TABLE OF CONTENTS.....	iv
1. LISTS OF ACRONYMS, FIGURES, AND TABLES.....	vi
1.1 List of Acronyms .....	vi
1.2 List of Figures .....	viii
1.3 List of Tables .....	x
2. EXECUTIVE SUMMARY.....	1
3. INTRODUCTION .....	3
4. BACKGROUND .....	4
5. RESULTS AND DISCUSSION .....	5
5.1. Project Management .....	5
5.1.1. Scope.....	5
5.1.2. Summary of Methods.....	5
5.1.3. Results.....	5
5.2. Characterization of materials recovered from pilot scale pyrolysis unit.....	6
5.2.1. Scope.....	6
5.2.2. Summary of Experimental Methods .....	6
5.2.3. Results.....	8
5.3. Preforming of Recycled Composite Fibers—Part A: BMC Production and Preliminary Molding ..	9
5.3.1. Scope.....	9
5.3.2. Summary of Experimental Methods .....	10
5.3.3. Results.....	10
5.4. Preforming of Recycled Composite Fibers—Part B: Composite Thermoplastic Compounding....	11
5.4.1. Scope.....	11
5.4.2. Summary of Experimental Methods .....	12
5.4.3. Results.....	13
5.5. Preforming of Recycled Composite Fibers—Part C: 3D Printable Resin Development .....	19
5.5.1. Scope.....	19
5.5.2. Summary of Experimental Methods .....	20
5.5.3. Results.....	20
5.6. Expanded TEA and LCA of rGF and rCF .....	23

5.6.1. Scope.....	23
5.6.2. Summary of Experimental Methods .....	23
5.6.3. Results.....	25
5.7. Recycled Composite Demonstration Part Fabrication—Part A: Automotive Vehicle Part Molding Trials .....	29
5.7.1. Scope.....	29
5.7.2. Summary of Experimental Methods .....	29
5.7.3. Results.....	31
5.8. Recycled Composite Demonstration Part Fabrication—Part B: BAAM Composite Development and Test Part Analyses.....	34
5.8.1. Scope.....	34
5.8.2. Summary of Experimental Methods .....	34
5.8.3. Results.....	35
6. BENEFITS ASSESSMENT .....	38
7. COMMERCIALIZATION .....	39
8. ACCOMPLISHMENTS .....	40
9. CONCLUSIONS.....	41
10. RECOMMENDATIONS.....	42
11. REFERENCES .....	43

# 1. LISTS OF ACRONYMS, FIGURES, AND TABLES

## 1.1 List of Acronyms

ABS	Acrylonitrile Butadiene Styrene
ACCE	Automotive Composites Conference & Expo
ACMA	American Composites Manufacturers Association
ASME	American Society of Mechanical Engineering
BAAM	Big Area Additive Manufacturing
BMC	bulk molding compound
BPA	bisphenol A
BT	battery tray
CAD	computer aided design
CAMX	Composites and Advanced Materials Expo
CAPEX	Capital Expenditure
CCS	Carbon Conversion Solutions
CF	carbon fiber or cash flow
CHZ	CHZ Technologies, Inc.
CI	Capital Intensity
CNAM	Composite and Nanocomposite Advanced Manufacturing-Biomaterials Center
CNC	Computer Numerical Control
CT	computed tomography
DiFTS	discontinuous fiber thermoplastic sheet
DMA	dynamic mechanical analysis
DOD	Department of Defense
DOE	Department of Energy
EC	energy credit
ECM	extrusion-compression molding
EOL	end of life
EPRI	Electric Power Research Institute
FOA	Funding Opportunity Announcement
FP	finished product
GE	General Electric
GF	glass fiber
HDPE	high density polyethylene
ICM	injection compression molding
IM	injection molding
IMECE	International Mechanical Engineering Congress and Exposition
IR	infrared
IRR	Internal Rate of Return

кта	kilotons per annum
KUG	KUG GmbH
LCA	life cycle assessment
LDPE	low density polyethylene
LFT	long fiber thermoplastics
MSW	municipal solid waste
NE	net energy
NPV	Net Present Value
OC	Owens Corning
PBT	polybutylene terephthalate
PC	polycarbonate
PCR	Post-Consumer Recycled
PCT	Patent Cooperation Treaty
PP	polypropylene
rCF	recovered carbon fiber
rGF	recovered glass fiber
RM	raw material (composite EOL scrap)
ROCC	Return on Corporate Capital
SAMPE	Society for the Advancement of Material and Process Engineering
SDSMT	South Dakota School of Mines and Technology
SEM	scanning electron microscope
SMC	sheet molding compound
TE	total energy
TEA	techno-economic analysis
T <sub>g</sub>	glass transition temperature
TGA	thermogravimetric analysis
UT	University of Tennessee
UTM	Universal Test Machine
VOC	volatile organic compound
XIRR	Extended Internal Rate of Return

## 1.2 List of Figures

Figure 1. Shredding sequence for converting wind blade end of life materials, originating from GE Renewable Energy, into Thermolyzer™ feedstock. ....	7
Figure 2. Example image of Thermolyzer™ recovered glass fiber/char mixture from wind blades. ....	7
Figure 3. Example of a single filament mounted during tensile testing.....	8
Figure 4. Measured average fiber Weibull characteristic fracture strengths for virgin fiber, rGF from Phase II (current phase), and rGF from Phase I (previous report IACMI/R004-2020/6.4). Error bars represent estimated sample standard error. ....	9
Figure 5. TGA experimental results on fiber bundle specimens taken from the bulk recovered fiber/char mix in Figure 2.....	9
Figure 6. Burn off cleaned fiber used in BMC production. ....	10
Figure 7. Summarized results as function of rGF to virgin fiber in an automotive forward lighting BMC. ....	11
Figure 8. Char covered pyrolyzed fiber before (on left) and after (on right) high temperature burn off in ambient atmosphere. ....	13
Figure 9. Fiber recovered after sonication indicating noticeable char removal although more impurities remaining when compared versus high temperature burn off.....	14
Figure 10. Nonwoven mats stacked in press prior to compression molding.....	14
Figure 11. Consolidated LDPE composite test panels after compression molding procedure: burn off fiber panel on left appears white while sonicated fiber panel on right appears black. ....	14
Figure 12. Summarized mechanical test results on wetlay nonwoven LDPE composites with 30 wt% rGF versus virgin LDPE.....	15
Figure 13. Observed specimen fracture in tensile testing reveals failure through fiber separation in remaining char coated bundles.....	15
Figure 14. Example bicycle stem geometry molded from LDPE nonwoven mats and burn off rGF after basic polishing and painting.....	16
Figure 15. Summarized results as function of rGF to virgin fiber in an electrical BMC.....	16
Figure 16. Cyclone Separation system and cleaned fiber .....	17
Figure 17. SEM image of fracture surface of an rCF PA6 composite. ....	18
Figure 18. Mechanical properties of PA6 composites containing Thermolyzer™ carbon fibers and virgin carbon fibers as a function of fiber loading level.....	19
Figure 19. TGA curves of neat ABS and rGF/ABS composite. ....	21
Figure 20. Temperature dependence of storage moduli (left) and tan $\delta$ (right) of neat ABS and recycled glass fiber/ABS composite.....	21
Figure 21. SEM images of fracture surfaces of neat ABS (A and B) and rGF/ABS composite (C and D) at two different scales of 200 $\mu\text{m}$ and 20 $\mu\text{m}$ . ....	22
Figure 22. CAD rendering of the seat back rest tool cavity (left) and core (right). The tool is approximately 76 cm $\times$ 45.7 cm $\times$ 35.6 cm and weighs $\approx$ 910 kg. ....	29

Figure 23. Processing sequence of infrared (IR) heating of the rCF-PA66 mat and transfer to the press for compression molding. Left to right: IR heating of rCF-PA66 in conveying oven; transfer heated rCF-PA66 to press (tool); 5-min cycle time and demold; and back side of the part. .... 30

Figure 24. Vacuum thermoforming machine and tool used to mold the John Deere door panel..... 31

Figure 25. SMC seat back rest seats: (a) the charge placement was optimized for cycle time 3 minutes with no visible defects; (b) the flash is marginal, which can be eliminated in production with a sharper shear edge; and (c) thickness profile of the seat back was consistent. Future parts can use rGF-vinyl ester bulk charge and mold in a similar fashion. .... 32

Figure 26. Representative battery tray cover parts made from rCF-PA66 and rCF-epoxy. The parts look very similar for both materials. (a) short shot in IM of rCF-PA66 and (b) fully filled part..... 32

Figure 27. Vacuum thermoformed door panel part, molded from a rCF/rGF mixture in an 80:20 HDPE/PP matrix. (The HDPE was a recycled polymer). .... 34

Figure 28. Left: Change in complex viscosity as a function of the angular frequency of neat ABS and rGF/ABS composite (rGF/ABS) at 220 °C. Right: Change in storage modulus as a function of the angular frequency of neat ABS and rGF/ABS composite (rGF/ABS) at 220 °C. .... 35

Figure 29. XCT analysis: the distribution of pores segmented from the low magnification scan for the 3D-printed part. .... 36

Figure 30. XCT analysis: the 3D images that showed the segmented glass fibers for the 3D-printed part. .... 36

Figure 31. XCT 3D-printed part. .... 37

Figure 32. Summary of Embodied Energy (EE) Distribution (left) and Recycled EE Savings (right). .... 38

### 1.3 List of Tables

Table 1. Mechanical properties of PA6 composites containing rCF and other recycled and virgin carbon fibers at fiber loading levels of 15 wt% (left) and 20 wt% (right). .....	18
Table 2. Comparison of tensile properties for neat ABS, rGF/ABS composite, 3D-printed parts .....	22
Table 3. Mass/Energy Balance from Project 6.4 using CHZ Pilot line to process commercially supplied composite EOL/Scrap (Cases 1 to 4) .....	24
Table 4. Financial summary of the full investment case of \$58.5mm CAPEX at different RM costs and FP Values .....	26
Table 5. Payback vs value at different cost levels for full investment case (\$58.5mm) .....	27
Table 6. CAPEX and CI at Various RM Capacities .....	27
Table 7 (left). Financial summary for shared investment case (~20% of full CAPEX = \$11.5 mm) at different RM costs and FP Values .....	28
Table 8 (right). Payback vs value at different cost levels for shared investment (20% of full CAPEX = \$11.5mm) case .....	28
Table 9. Preliminary mechanical test data of rCF thermoplastics and thermosets compared to long fiber virgin and textile grade carbon fiber thermoplastics.....	33
Table 10. Mechanical properties of the HDPE and HDPE/PP composites reinforced with rGF, rCF and rGF/rCF mixture. ....	33

## 2. EXECUTIVE SUMMARY

The goal of this IACMI Phase II Technical Collaboration Project was to establish the viability of producing affordable, recycled composite parts, which were produced from fibers with the properties in the range of those reclaimed through the controlled pyrolysis technology demonstrated in Phase I [1]. For the purpose of this report, we use the terms “recovered carbon fiber” (rCF) and “recovered glass fiber” (rGF) as the material reclaimed from controlled pyrolysis. This fiber recycling technology utilizes the inherent energy in composites for fuel and preserves the structural value of glass fiber (GF) and carbon fiber (CF) for reuse. It can also be used for recycling other waste streams at the same facility, thus spreading capital risk and recovery across multiple industries and achieving economy of scale. A second goal to be addressed was the viability of using recycled fibers as reinforcing materials in additive manufacturing applications.

The project scope was to evaluate and validate demonstration of recycled composite parts and preforms that show the potential for successful business cases built around recycled composite products. The ultimate vision of the Phase II project is to enable widespread adoption of recycled materials throughout the U.S. and contribute significantly to the Institute’s technical goal of 80% composite recycling in five years.

The American Composites Manufacturers Association (ACMA) led the project, with participation from the University of Tennessee (UT), South Dakota School of Mines and Technology (SDSMT), LyondellBassell, Owens Corning (OC), and CHZ Technologies (CHZ). This report summarizes the scope, experimental methods, and results of the following activities:

- Characterization of materials recovered from pilot scale pyrolysis unit
- Preforming of Recycled Composites Fibers:
  - Part A – Bulk Molding Compound (BMC) Production and Preliminary Molding
  - Part B - Composite Thermoplastic Compounding
  - Part C – 3D Printable Resin Development
- Expanded Techno-Economic Analysis (TEA) and Life Cycle Assessment (LCA) of rCF and rGF
- Recycled Composite Demonstration Part Fabrication
  - Part A – Automotive Vehicle Part Molding
  - Part B – Big Area Additive Manufacturing (BAAM) Composite Development and Test Part Analyses

In addition, the report presents the benefits, commercialization, accomplishments, conclusions, and recommendations of the potential for recycled parts using rCF and rGF.

In the experimental portion, the following significant results were obtained:

- Overall, this project proved the potential of recycling fibers in various composite applications recovered using the pyrolysis route at up to 20% substitution of virgin glass and carbon fiber. Additional work should focus on removal of char and tighter control of the thermal history of the recycled fibers.
- *In BMC compounds*, supplementing the rGF with just a low level (10-20%) of virgin fiber, maintains a moldable compound with little property loss in flexural and tensile strength.
- *In low density polyethylene (LDPE)/rGF composites* (comingling process), following a post-pyrolysis process to remove the surface char, good fiber/resin dispersion was observed throughout the composite in several test parts. This suggests that wet-lay manufacturing may be an ideal pathway for forming composite intermediates from rGF.
- *In PA6/recycled CF composites* (DiFTS process), at fiber loadings of just 30 wt%, the flex strength reaches about 250 MPa and the tensile strength 180 MPa, suggesting commercial value.

- *In 3D printed resin development*, compared to neat ABS, the compression-molded rGF/acrylonitrile butadiene styrene (ABS) composite showed a 20% higher tensile strength and a 110% higher Young's modulus, proving the reinforcing effect of rGF.
- *Recycled demonstration composite parts* were produced with rGF and rCF, using various resins and processes, and compared to those made with virgin fibers, with favorable results:
  - Seat back rest
  - Battery tray part
  - John Deere door panel
  - Submersible device generated using 3D printable composite feedstock material

Finally, the TEA/LCA presented several business cases toward IACMI's goal of 80% recycling.

This project created a new, valuable knowledge base around conventional pyrolysis that can be built upon to spur new advances. Two companies are actively pursuing commercialization of controlled pyrolysis systems:

1. A commercial pyrolysis unit has been permitted and site prep started in Youngstown, OH by CHZ Technologies, Inc to process tires which is anticipated to be in operation by early 2023. Testing is in process for electronic scrap, treated railroad ties/utility poles, and other materials. Funding for a further demonstration system dedicated to composites is being pursued with a combination of public and private support.
2. In a separate development, a pyrolysis-based process is now being scaled up in Knoxville, TN by Carbon Rivers LLC to focus on recovery of fiberglass from wind blades and other composite materials. While this company uses a different pyrolysis process from the one examined in this study, the technoeconomic and lifecycle assessment frameworks and identification of key differentiating limitations in conventional pyrolysis have supported the value proposition of this new process as it moves towards commercialization with composites industry partners.

### 3. INTRODUCTION

This Technical Collaboration Project further provided a framework for technology commercialization and quantifying the recyclability of selected composites. The project demonstrated a mechanical and thermal recycling approach that captures value for energy content and the residual ash/fiber. Specifically, this collaboration project validated and demonstrated how rGF and rCF obtained through controlled pyrolysis can be postprocessed and reincorporated into second generation thermoset and thermoplastic preforms, which themselves can be used to mold new Original Equipment Manufacturer (OEM) parts, such as for the automotive industry. The unknowns that were determined included the physical and structural properties of second generation molded and additively manufactured polymer composites containing rCF and rGF. Targeted applications were examined that have the potential for sustainable reuse.

In addition to technology development, the TEA demonstrated the ability to quantitatively assess intermediate progress towards its goal of 80% composite recyclability in 5 years.

## 4. BACKGROUND

Composite materials deliver compelling energy savings and other sustainability benefits during manufacture and operational life. However, at end-of-life, due to their robustness, composite materials are difficult to recycle or re-use, contributing to a perception that composites are inferior to competing materials in terms of cradle-to-cradle sustainability. Many high-volume composites also impose significant, direct waste handling costs at end-of-life. Corporate sustainable sourcing policies may limit composites from being adopted as fully as they otherwise might.

In addition to their robustness, the diversity of composites makes recycling challenging. The composite materials industry is a large, fragmented, multi-tiered, multi-material industry employing millions of workers across the U.S. economy. Many composites manufacturers are small to medium size businesses. This diverse nature represents a key barrier to finding a universal, effective recycling solution. There are thousands of composite applications where component parts are produced in large and small facilities across the country. In addition to repair technologies to extend the life of composite materials, potential recycling opportunities abound: recycling or reusing fibers, yarns and mats; managing thermoset resin waste; reprocessing scraps and trimmings produced in parts manufacture; and post-use reclamation, recycling, recovery of materials and energy using the cement kiln route, repurposing of composite parts in alternative applications, and remanufacturing of composite parts for new applications. The key to achieving a viable business case for recycling these materials is to establish and demonstrate the capturable value of these various waste streams. Mechanical and other material properties of recycled composites need to be matched with appropriate target applications to educate both industry and consumers as to the uses of recycled composite materials. This knowledge can stimulate demand for additional recycled composite materials and help bootstrap this nascent materials industry.

The February 2016 IACMI Roadmap [2] and Summary [3] included the comment, “There is concern about the reality of the goal of 80% composite recyclability into useful products.” This statement clearly shows the need for an adaptable and robust composite recycling technology in the U.S., as well as a framework for incorporating recyclability from different stages in the value and supply chain to document progress towards the 80% goal.

## 5. RESULTS AND DISCUSSION

### 5.1. Project Management

#### 5.1.1. Scope

This task provided for the tracking of the project outcomes with respect to the stated deliverables and milestones. Furthermore, this task provided the required financial and schedule reporting to Recipient and to DOE to ensure compliance with the project objectives and the goals of the Institute and the Funding Opportunity Announcement (FOA).

#### 5.1.2. Summary of Methods

As the lead organization, ACMA requested and compiled monthly progress reports from team members and held monthly meetings with project team members (more often when needed) to coordinate activities.

#### 5.1.3. Results

All deliverables and milestones of the project were met, although some target deadlines were delayed due to lab closures from COVID-19. Under ACMA coordination, the deliverables/milestones included:

- *Milestone 6.29.1.1* - ACMA coordinated communications between project team and non-IACMI composite recycling activities running parallel to 6.29 relevant to project activities (e.g. TEA, etc.). *ACMA*
- *Milestone 6.29.2.1* - The results of pyrolyzed fiber characterization before and after potential char removal were reported to the project team and DOE for review. *UT*
- *Final Milestone 6.29.1* - A source of pyrolyzed fiber feedstock without metallic (or other showstopper) contamination and sufficiently intact mechanical properties was made available to the rest of the project development team. *CHZ*
- *Final Milestone 6.29.2* - The baseline properties (strength and stiffness) and processability of the chopped fiber composite preforms were established and reviewed against potential composite part applications. *UT*
- *Milestone 6.29.3.1* - Results were reported to DOE on BMC production and preliminary molding with the recovered fiber. *LyondellBassell*
- *Milestone 6.29.3.2* – Results were reported to DOE of composite thermoplastic compounding with the recovered fibers. *UT*
- *Milestone 6.29.4.1* - Final report was briefed to DOE on the TEA and the business case options.
- *Milestone 6.29.5.1*- Results of the automotive vehicle part molding trials were reported to DOE. *A Schulman, ACMA, UT, LyondellBassell, ACMA, UT*
- *Milestone 6.29.5.2* - The results of BAAM composite development and test part analyses with the recovered fibers were reported to DOE. *ORNL*

## 5.2. Characterization of materials recovered from pilot scale pyrolysis unit

### 5.2.1. Scope

Previously, ~1000 lbs. of pre-shredded glass fiber composite scrap was pyrolyzed on site at CHZ/KUG in a pilot scale process in Forst, Germany using time-temperature information learned earlier from IACMI Project 6.4 [1]. The materials had been processed via controlled pyrolysis, capturing the synthesis gas samples and the char containing the fibers. The synthesis gas and char samples from the Pilot Tests were sent to an analytical lab for mass and energy balance, synthesis gas and char analysis, volatile organic compound (VOC) measurement, and testing for the presence of halogens in the synthesis gas and char. Analytical tests for halogenated dioxins and furans were completed only if halogens were present in either the gas or the char. The output char was also checked to ensure no contaminants, such as metallic debris that could prevent further processing, were present. A full report for previous Project 6.4 was presented to the project team, and the residual char containing the fibers was shipped back to the US testing facility from Forst, Germany for characterization and fiber post processing. The pyrolyzed fiber batches were placed in sealed super sacks, shrink wrapped, and banded onto an international shipping pallet. Care was taken to ensure material used to start/complete the pyrolysis process (i.e., not processed at normal steady state conditions) was segregated from core representative material.

In this task, the reclaimed glass fibers from the pyrolysis pilot tests in Forst, Germany were sent back to the project team in the U.S. for characterization. The as-received recycled glass fibers were examined using techniques such as scanning electron microscopy (SEM) and X-ray photoelectron spectroscopy. Mechanical properties (strength, stiffness, and failure strain) were determined using single fiber tests.

The project team also assessed the effects of char removal through burn off (and other alternatives) to examine the tradeoff of a pure recycled product at the expense of increased fiber damage. Char removal thermal profiles were established via thermogravimetric analysis (TGA) followed by single filament mechanical testing.

### 5.2.2. Summary of Experimental Methods

Approximately 1000 lbs. of end-of-life wind blade fiberglass composite material was supplied by GE Renewable Energy for project research. CHZ Technologies, working with a commercial shredding subcontractor, put the incoming blade pieces through a two-pass shredding process (Figure 1) to get the materials broken down into nominally 2" inch chip sizes with a final yield of ~700 lbs. The shredded material was then shipped to CHZ Technologies' partner KUG's pilot pyrolysis reactor facility in Germany. The incoming material was processed in 2 rounds: a temperature range finding sweep followed by processing at observed ideal conditions. Prior to processing, the pyrolysis reactor was thoroughly cleaned out to avoid cross contamination of recycled fiber with metals, etc. from previous research projects performed at the site. This cleaning step was especially important as metal contamination had been a limiting factor in materials research during Phase I of the project. After processing, ~100 lbs. of pyrolysis recovered fiber/char mixture was shipped back the US for further study.



Figure 1. Shredding sequence for converting wind blade end of life materials, originating from GE Renewable Energy, into Thermolyzer™ feedstock.

Visual inspection of the pyrolyzed fiber provided by CHZ Technologies in Figure 2 indicated the presence of intact, recovered glass fiber coated and mixed with loose carbon char alongside wood chips used to plasticize / force the original input composite shreds to flow through CHZ Technologies' continuous pyrolysis reactor design. One metal object was detected in the visually inspected specimen; however, metal/other contamination was well below specimens received during the project's earlier phase and appeared to be at an acceptable level for lab scale composite development. Direct measurements on the charred fiber bundles indicated an average recovered fiber length of approximately 1.8" although lengths varied from 1.4"- 2.8".

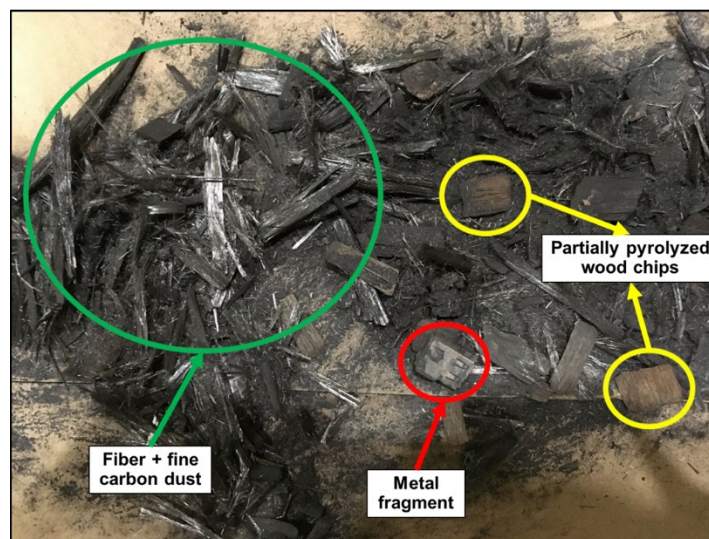
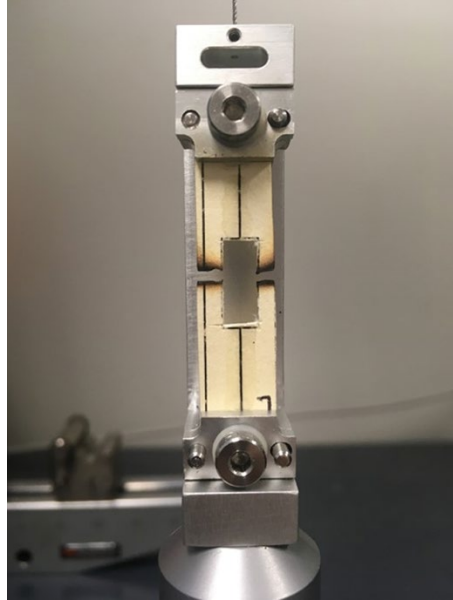


Figure 2. Example image of Thermolyzer™ recovered glass fiber/char mixture from wind blades.

Individual filaments recovered from the pyrolyzed glass fiber were subjected to tensile testing based on ASTM C1557 to gauge mechanical quality. Testing was carried out on a TestResources 313 Series Electromechanical Universal Testing Machine (UTM) equipped with a 5N load cell after mounting the specimen via paper tab (Figure 3). Testing was carried out via a constant displacement rate of 0.2mm/min on a fiber gauge length of 12.7mm (0.5") after preloading each filament to 0.03N. Each individual filament's average diameter for stress calculations was measured via optical microscopy prior to mechanical testing, with overall average filament diameter measuring 15.4µm and standard deviation 1.9µm. To account for the brittle nature of glass, the fiber strength measurements were subjected to a commonly used Weibull analysis, described in [4], to determine a characteristic fiber strength. While the exact virgin E-glass fiber used in original wind blade construction was unavailable, a surrogate sample of commercial virgin fiber already on hand was tested as a stand-in for virgin versus recycled fiber strength performance.



*Figure 3. Example of a single filament mounted during tensile testing.*

### 5.2.3. Results

The data in Figure 4 indicates that the rGF exhibited a tensile strength -65% below virgin fiber performance, appearing slightly better than fiber recovered during the project's earlier phase. The strength degradation is caused by abrasion of the fiber surface (i.e., rubbing of the fiber against other surfaces), which causes tiny scratches to form on the surface of the glass. Failure of GF due to surface flaws is well established. While most of the fiber in a wind blade does not go through the same intermediate forming process as in SMC, the fiber will invariably rub against different surfaces during high-speed production of the fabrics used in blade construction and so some damage should be expected. The cause of the degradation is not specific to SMC production and therefore not necessarily limited to SMC. Similar tests on the production process for the intermediates used to build the blade are needed to determine this factor.

It is also worth noting that previous work examining the GF strength timeline in automotive SMC manufacturing revealed how the GF lost -27% tensile strength during original composite manufacturing / in service use before recycling, and so it is unlikely pyrolysis was responsible for the full -65% strength decline. [5]

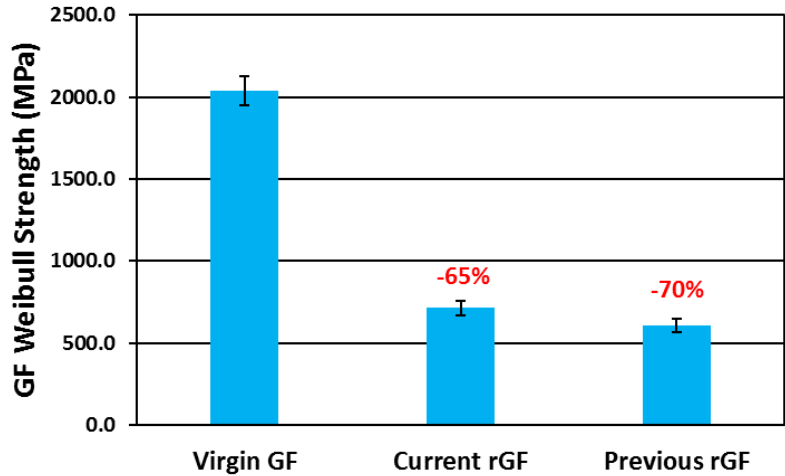


Figure 4. Measured average fiber Weibull characteristic fracture strengths for virgin fiber, rGF from Phase II (current phase), and rGF from Phase I (previous report IACMI/R004-2020/6.4). Error bars represent estimated sample standard error.

Beyond the glass fiber itself, a significant portion of recovered sample weight existed as carbon char. Bulk fiber/char mixture burn off tests in a furnace, weighing before and after, indicated a recoverable 35-40% fiber weight overall. TGA tests on the charred fiber directly (Figure 5) indicated only ~4.3 wt% of char was coated directly on the glass fiber surfaces, with measured values varying ~2-9 wt%.

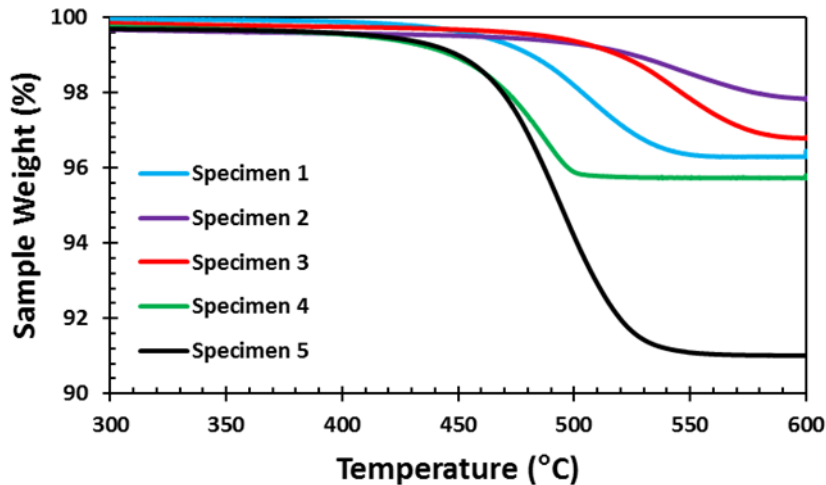


Figure 5. TGA experimental results on fiber bundle specimens taken from the bulk recovered fiber/char mix in Figure 2.

### 5.3. Preforming of Recycled Composite Fibers—Part A: BMC Production and Preliminary Molding

#### 5.3.1. Scope

Pilot-scale BMC compounding trials evaluated the rCF and rGF and assessed their impact on (a) physical handling characteristics, impact on mixing, etc.; (b) mechanical properties of molded BMC and resulting physical characteristics of compared to product with virgin fibers; and (c) rCF and rGF in combination

with virgin fibers to determine trade-offs in properties. The mechanical properties were assessed against existing application demands for BMC, which were reported to the project team. In cases where further increases in mechanical performance was necessary for the recycled composite to meet minimal application needs or to increase the number of viable commercial applications as previously assessed, fiber surface treatments were also applied, such as new sizing coupling agents or binders, to determine the performance cost-benefit of additional fiber treatment.

### 5.3.2. Summary of Experimental Methods

To feed the rGF into a lab scale dispersion blade mixer BMC process, the fiber/char mixture first needed to have the bulk of the char and wood chip components removed. This was accomplished by heating the material in ambient atmosphere to 400°C for 1.5 hours followed by mechanical sifting with a 3-mesh screen. This process had a yield of nominally 35-40%, producing fiber feedstock as exhibited in Figure 6. This material was then mixed into two different BMC formulations: one for automotive forward lighting (16 wt% glass content) and one for electrical switch gears (25 wt% glass content). Different iterations of these BMCs were made varying recycled vs. chopped virgin glass fiber (1/4" lengths) content ratio as well as with and without a silane coupling agent added to the resin during mixing. No silane was added to the pure virgin glass fiber control specimens, as these fibers have already been commercially coated with a coupling agent. Mixed BMCs were molded into test plaques and machined for mechanical testing.

Flexural, Tensile and Izod impact values were tested for the different BMC sample configurations based of ASTM D790, ASTM D638, and ASTM D256 (Method A), respectively.



*Figure 6. Burn off cleaned fiber used in BMC production.*

### 5.3.3. Results

It should be noted that the typically chopped GF matchstick bundle integrity is greatly compromised through the process. Approximately 25% of the glass still has some bundle integrity. The aspect ratio of the glass varies. There are fibers up to 2" in length down to 1/32" and a lot of variation between those lengths; the lab scale BMC process is incapable of breaking all these different lengths down. Even with the large differences in length, the fibers did process to an acceptable consistency in the BMC compound mixing.

Looking at the mechanical properties (Figure 7) and using n = 5 to 8 depending on the material and type of test, there are significant reductions in flex and impact as the amount of rGF is increased on both BMC resin formulations. This was apparent in compound produced with and without silane additive. Both flexural and tensile modulus in all compounds did not see as great of a loss with addition of the rGF. This is most likely due to the rigidity of the unsaturated polyester resin itself and the glass is not the major contributing factor to these properties. The most significant loss was to notched-Izod impact results, as in all cases this property was greatly reduced as the amount of rGF increased. Flexural strength exhibited a similar trend in behavior. Tensile strength showed less reduction but varied greatly between the two BMC types. The higher glass content electrical BMC saw greater reduction in tensile strength than did the lower content automotive BMC. Addition of a silane coupling agent improved tensile properties in both BMCs as compared to the non-silane batches. At a 1:4 wt ratio of rGF to virgin fiber content, both BMCs showed property losses that were relatively low and deemed not significant in some instances by our statistical analysis. Based on this performance, a low level (10-20%) replacement of virgin fiber in these BMC compounds with rGF is possible while still maintaining a moldable compound with little property loss. The biggest challenge remains cleaning of the fiber to acceptable levels for BMC processing and the yield from said cleaning. The economics of this would need to be evaluated to see the cost impact.

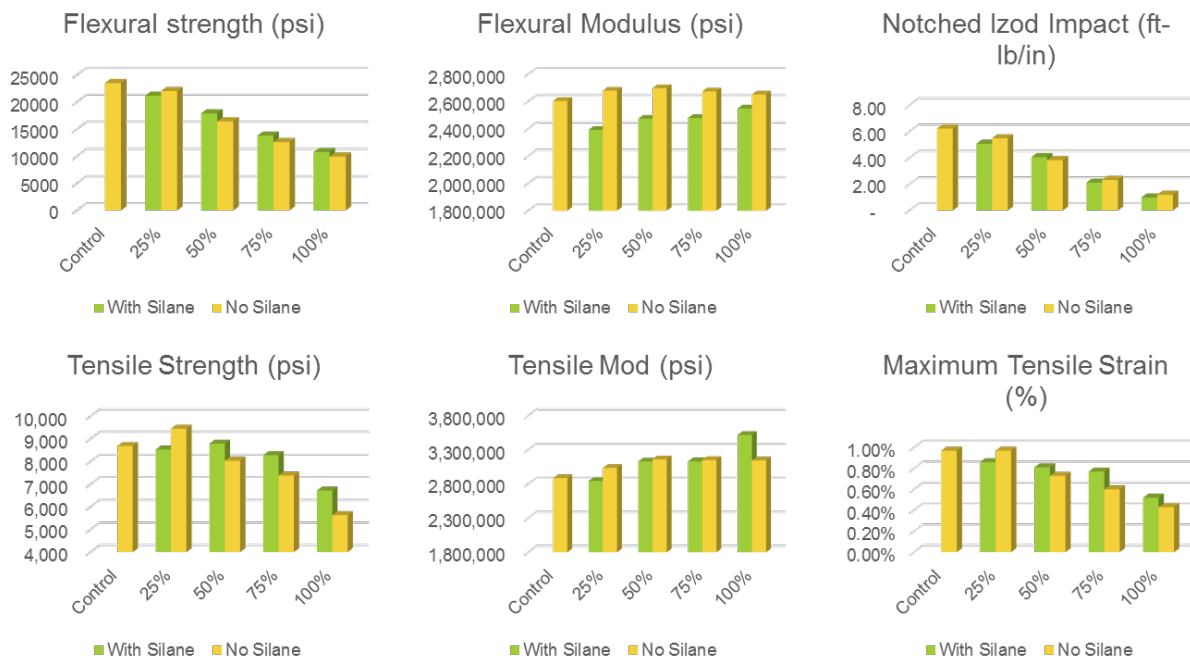


Figure 7. Summarized results as function of rGF to virgin fiber in an automotive forward lighting BMC.

## 5.4. Preforming of Recycled Composite Fibers—Part B: Composite Thermoplastic Compounding

### 5.4.1. Scope

The following aspects of composite thermoplastic compounding were studied:

- (a) LDPE/recycled glass fiber composites (comingling process)
  - Comingling of LDPE fiber with rGF into nonwoven thermoplastic prepreg
  - rGF post-process cleaning

- Wet-lay forming & compression molding
- LDPE / rGF composite performance

(b) PA6/rCF composites (DiFITS process) [6,7]

- Cleaning of rCF and removal of char using a cyclone method.
- Discontinuous fiber thermoplastic sheet (DiFITS) processing of rCF in a PA6 resin.
- Mechanical performance of laminated PA6/rCF sheets

#### 5.4.2. Summary of Experimental Methods

(a) LDPE/rGF composites (comingling process)

- ***Comingling of LDPE fiber with rGF into nonwoven thermoplastic prepreg***  
Composite tensile and flexural material properties were measured based on ASTM D3039 and ASTM D790, respectively. Testing was carried out on a TestResources 313 Series Electromechanical UTM equipped with a 10kN load cell. For reference pure, LDPE fiber mats were made, compression molded, and mechanically tested as well for baseline plastic performance comparison.
- ***Pyrolyzed fiber post-process cleaning***  
Two routes were attempted to reduce the char content of the as-received rGF: high temperature burn off and bath sonication. In the burn off approach, the charred rGF was hand separated from the bulk mix and placed in a furnace at 450°C for 3hr. After reacting with oxygen in the ambient atmosphere, the resulting de-charred rGF had a yield of approximately 88%. The fiber was visually much cleaner (Figure 8) after processing but still exhibited an off-white coloration. In the sonication approach, the charred fiber was placed in a sonication bath at the maximum power setting with the bath heated to 80°C overnight.
- ***Wet-lay forming & compression molding***  
After post-process cleaning, the rGF from both processes was mixed with chopped LDPE fiber (1/4" length) using a lab scale wet-lay mixing box to produce 70% LDPE / 30% glass fiber ratio (~320gsm) 12" x 12" mats. Twelve mats were then stacked one on top of the other and compression molded between heated caul plates to consolidate then into composite test panels (shown later in Figure 10). Compression molding was accomplished via the following method: (1) 12 consecutive nonwoven mats stacked and placed in press, (2) Caul plates heated to 145°C over 30 minutes, (3) nonwovens allowed to absorb heat for another 30 minutes without tonnage, (4) 5 tons of pressure applied for 15 minutes, (5) consolidated panel cooled to room temperature over 30 minutes before demolding.
- ***LDPE / recycled glass fiber composite performance***  
Composite tensile and flexural material properties were measured based on ASTM D3039 and ASTM D790, respectively. Testing was carried out on a TestResources 313 Series Electromechanical UTM equipped with a 10kN load cell. For reference pure, LDPE fiber mats were made, compression molded, and mechanically tested as well for baseline plastic performance comparison.

(b) PA6/recycled carbon fiber composites (DiFITS process)

- ***Cleaning of rCF and removal of char using a cyclone method***  
A cyclonic separation method was developed to remove impurities (metal, wood, etc.) and separate loose char from the rCF. Experiments were carried out with the help of two industrial

vacuum system and custom designed cyclone setup (shown later in Figure 16).

- ***Discontinuous fiber thermoplastic sheet (DiFTS) processing and composite lamination***  
Sheets of PA6 incorporating rCF at two different loading levels (15 wt% and 20 wt%) were produced using the DiFTS (Discontinuous Fiber Thermoplastic Sheet) manufacturing process [6,7] developed by the Composite and Nanocomposite Advanced Manufacturing-Biomaterials Center (CNAM) at SDSMT. The composite sheets (about 0.7mm thick) were then consolidated to ~3.5mm thick laminates in a vacuum forming process.
- ***PA6 /rCF DiFTS performance***  
The tensile strength and modulus of the laminates were tested according to ASTM D638, and the flexural strength and modulus of the laminates were tested according to ASTM D790.

### 5.4.3. Results

#### **(a) LDPE/recycled glass fiber composites (comingling process)**

- ***Comingling of LDPE fiber with rGF into nonwoven thermoplastic prepreg***  
The starting load of carbon char was too high for immediate wetlay processing, so additional post-pyrolysis processing was done to further purify the rGF.
- ***rGF post-process cleaning***  
The fiber recovered in this method still retained a fair amount of surface char (Figures 8, 9); however, there was visual evidence in Figure 9 of some surface char removal in addition to loose char removal.



Figure 8. Char covered pyrolyzed fiber before (on left) and after (on right) high temperature burn off in ambient atmosphere.



Figure 9. Fiber recovered after sonication indicating noticeable char removal although more impurities remaining when compared versus high temperature burn off.

- **Wet-lay forming & compression molding**

The resulting panels are shown in Figure 11, which shows two important points. First, in the test panel produced from burn off fiber, most char is indeed removed however, black segments of carbon char coated char are visible within the plate. These black sections were not visible in the specimens when being originally removed from the burn off furnace suggesting that outer layers of rCF bundles that had their char removed inhibited burn off deeper inside the fiber chips. That said, the panels themselves appeared to consolidate well with minimal visible bubbles, thermoplastic fibers, or other signs of failed consolidation. Mechanical test specimens were then CNC (Computer Numerical Control) machined out of each panel for characterization.



Figure 10. Nonwoven mats stacked in press prior to compression molding.



Figure 11. Consolidated LDPE composite test panels after compression molding procedure: burn off fiber panel on left appears white while sonicated fiber panel on right appears black.

- **LDPE / rGF composite performance**

As would be expected from the additional char contaminates, the sonicated fiber exhibited lower performance than burn off fiber; however, the sonicated fiber specimens still managed to exhibit noticeably elevated performance over pure plastic. While LDPE has very low starting properties resulting in larger performance gains than would be seen in a more engineering polymer system like nylon, the observed degrees of fiber reinforcement coupled with good fiber/resin dispersion throughout the composite suggests wet-lay manufacturing may be an ideal pathway for forming composite intermediates from rGF. Testing results from the TestResources 313 Series Electromechanical UTM equipped with a 10kN load cell are reported in Figure 12, which makes it readily apparent that the addition of rGF made a significant impact on the relatively low mechanical properties of pure LDPE.

Examination of the failed test specimens as shown in Figure 13 clearly indicated that specimen failure occurred during mechanical separation of remaining char coated fiber bundles running near perpendicular to the mechanical testing direction. This suggests further improvements in cleaning that allow better resin penetration and adhesion to the rGF could further improve performance, especially if also then treated with a conventional coupling agent like silane.

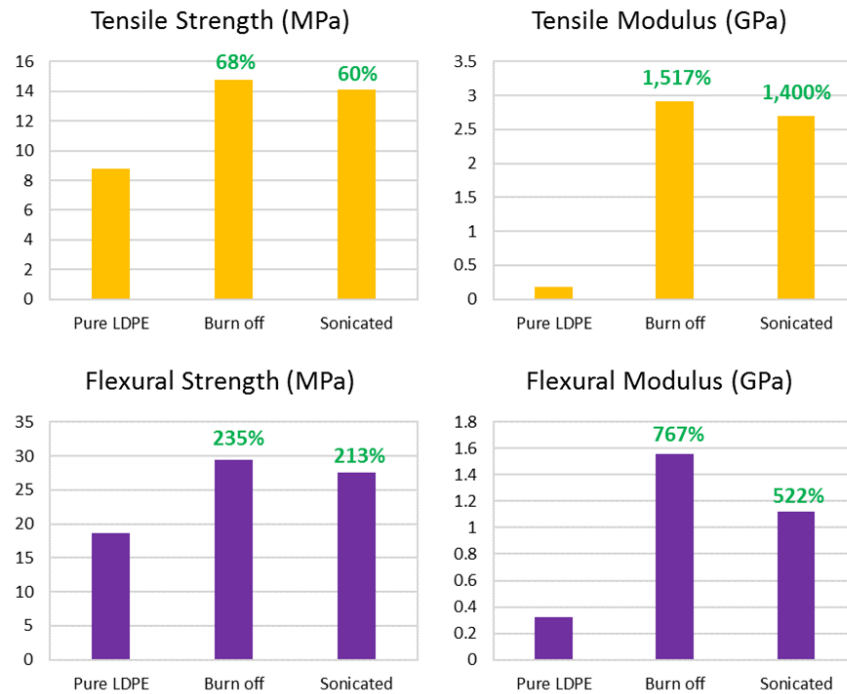


Figure 12. Summarized mechanical test results on wetlay nonwoven LDPE composites with 30 wt% rGF versus virgin LDPE.



Figure 13. Observed specimen fracture in tensile testing reveals failure through fiber separation in remaining char coated bundles.

To examine the potential for molding into parts with more complex, curved shapes, additional mats containing burned off rGF were made and molded into a prototype bike stem geometry using similar compression molding conditions to fabrication of the flat test panels. Despite the remaining charred masses still present, the comingled mats readily flowed in line with the mold's curvature with visibly good consolidation. The resulting prototype proved readily polishable and paintable producing the final part in Figure 14. Figure 15 shows the results as function of rGF to virgin fiber in an electrical BMC.



Figure 14. Example bicycle stem geometry molded from LDPE nonwoven mats and burn off rGF after basic polishing and painting.

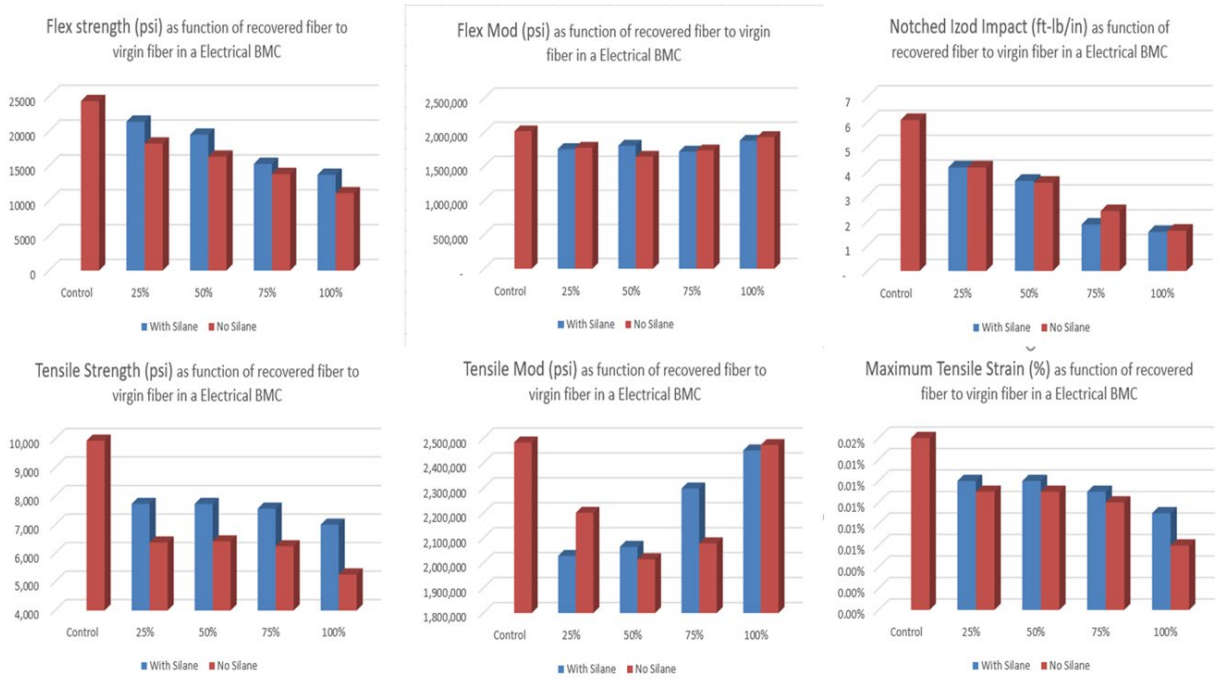


Figure 15. Summarized results as function of rGF to virgin fiber in an electrical BMC.

## (b) PA6/rCF composites (DiFTS process)

- ***Cleaning of rCF and removal of char using cyclone method***

An efficient cyclonic separation method was employed at SDSMT to remove metal and other heavy particulate contaminants from the Thermolyzer™-recycled fibers, without the use of filters (Figure 16). Denser particles in the air vortex have too much inertia to follow the tight curve of the stream, and thus strike the outside wall, and fall to the bottom of the cyclone chambers, where they can be removed. The fibers (being lighter) follow the tight curve of the stream and are pulled into the vacuum bag using the vacuum port. In addition, the loose char is found to accumulate on the sides of the vacuum bag, resulting in effective separation of much of the char from the fibers.

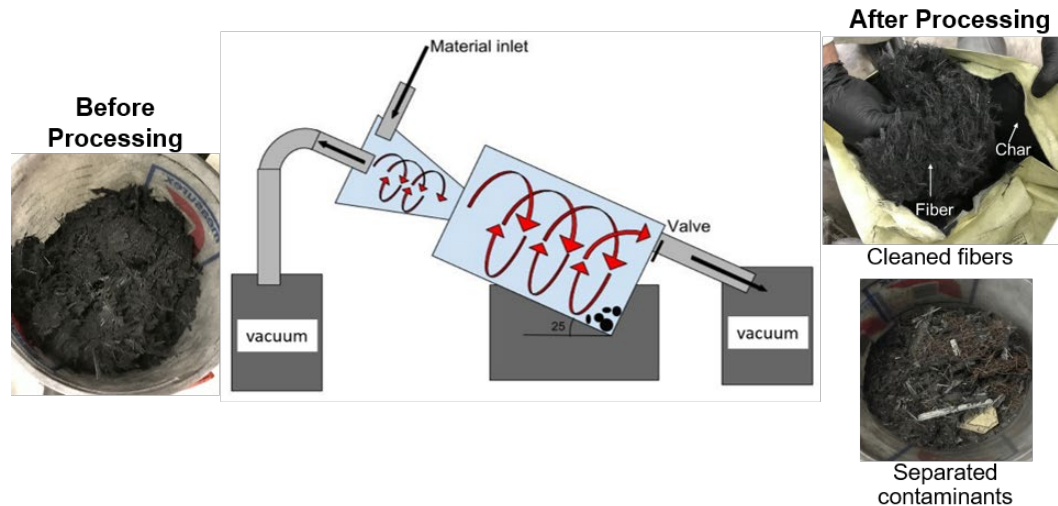


Figure 16. Cyclone Separation system and cleaned fiber

- ***Discontinuous fiber thermoplastic sheet (DiFTS) processing and composite lamination***

As mentioned in Experimental Methods above, composite sheets were produced and consolidated to ~3.5mm thick laminates in a vacuum forming process, which samples were then used to evaluate the mechanical properties and performance.

- ***PA6 /rCF composite performance***

The DiFTS process was used to incorporate the cyclone-cleaned CFs in a PA6 matrix at fiber loading levels of 15 wt% and 20 wt% (which includes any char still remaining in the fibers). The rCF was fed directly into the hopper of a 25mm twin screw extruder, without any further cleaning or application of sizing, and composite sheets (thermoplastic prepreg) were produced with a thickness of about 0.7mm. These sheets were then laminated into 3.5 mm thick plaques for mechanical property testing. As can be seen from Table 1, the flexure and tensile mechanical properties significantly increased after incorporating the rCF. At 20 wt% fiber loading, the tensile and flexural moduli both increased more than three times compared to the neat PA6; and the tensile and flexural strengths both increased by more than 50%. These results are shown in comparison with mechanical property data from composites comprising virgin carbon fibers and other recycled carbon fibers in the same PA6 matrix (all produced by the DiFTS process). Based on this result, the mechanical property enhancements are not as high for the rCF composites as for the other carbon fiber composites. However, the other recycled fibers in this case were recovered from (uncured) prepreg using a solvolysis process (Vartega fiber) or from waste fabric trim (SGL T40), rather than being recycled from an end-of-life product. Furthermore, no sizing was applied to the rCF that would improve fiber-matrix adhesion. SEM images of the broken surfaces, after tensile testing, show evidence of both fiber pull-out and well-embedded fibers in the rCF

composites (Figure 17). No attempt has been made to quantitatively analyze pull-out frequency in these composites relative to the other composites. It may also be noted that some residual char remained in the fiber bundles and attached to the fiber surfaces, so that the reported fiber loadings may be somewhat overestimated in the case of the rCF composites, leading to an underestimation of their properties at a given fiber loading.

Table 1. Mechanical properties of PA6 composites containing rCF and other recycled and virgin carbon fibers at fiber loading levels of 15 wt% (left) and 20 wt% (right).

Fiber	Fiber loading	Tensile		Flexure	
		Strength [MPa]	Modulus [GPa]	Strength [MPa]	Modulus [GPa]
None		87.2	4.0	129.4	3.7
Thermolyzer Carbon Fiber	15wt% (including char)	116.7	10.0	166.9	10.3
SGL T40 Recycled Carbon Fiber (Standard modulus)	15wt%	194.4	14.0	289.2	13.1
SGL Virgin Carbon Fiber (1/4" Standard Modulus)	15wt%	224.4	14.6	314.7	12.6
None		87.2	4.0	129.4	3.7
Thermolyzer Carbon Fiber	20wt% (including char)	137.6	13.0	203.8	13.3
SGL T40 Recycled Carbon Fiber (Standard modulus)	20wt%	225.5	17.8	305.9	15.4
Vartega Recycled Fiber (Standard Modulus)	20wt%	201.0	18.8	296.2	17.5
SGL Virgin Carbon Fiber (1/4" Standard Modulus)	20wt%	242.5	18.3	350.3	16.0

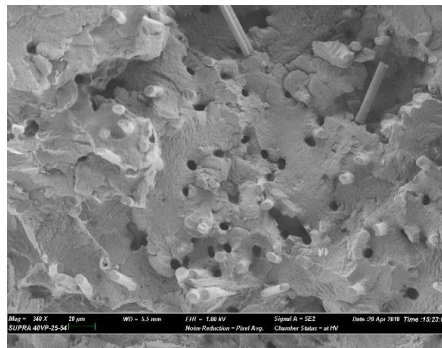


Figure 17. SEM image of fracture surface of an rCF PA6 composite.

The plots in Figure 18 show the effects of the fiber loading level on mechanical properties for the rCF PA6 composites compared to the virgin CF PA6 composites. While the properties for the rCF composites are lower than the virgin fiber composites, especially with respect to strength, the enhancements relative to the neat polymer are nevertheless of commercial value. Moreover, these plots suggest that at fiber loadings of just 30 wt%, both the flex modulus and tensile modulus of the rCF composites can be expected to exceed 20 GPa, while the flex strength and tensile strength should reach about 250 MPa and 180MPa respectively.

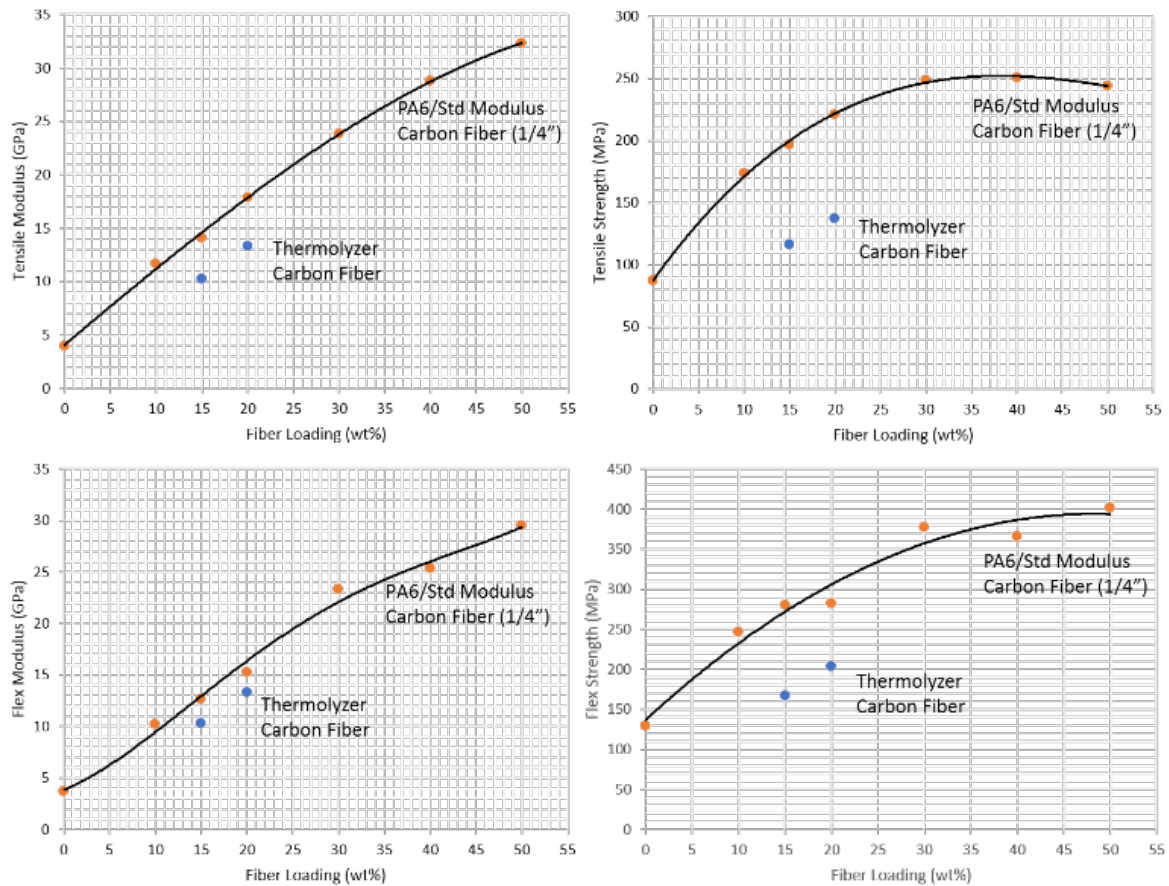


Figure 18. Mechanical properties of PA6 composites containing Thermolyzer™ carbon fibers and virgin carbon fibers as a function of fiber loading level.

## 5.5. Preforming of Recycled Composite Fibers—Part C: 3D Printable Resin Development

### 5.5.1. Scope

In this subtask, the project team oversaw development of 3D printable resin systems capable of directly producing new parts or molds that support part production from the rCF and rGF. The team conducted experiments to assess that printability and final part quality (such as mechanical properties, surface properties, rheology, etc.) remain aligned with the project objective of producing final demonstration recycled composite parts. Parts printed at this stage consisted of mechanical test specimen geometries and small basic shapes (e.g., planks) to assess shape stability. The project team also examined other composite preforming techniques to assess their potential for production of recycled composite preforms.

To gauge the mechanical properties of new, recycled thermoplastic composites, analyses were also conducted on compression molded and compounded mixtures (after high-shear compounding or twin-screw extrusion) using such techniques as TGA, dynamic mechanical analysis (DMA), or another method suitable for analyzing the flow behavior of polymers. Next, the mechanical testing specimens prepared from these mixtures were tensile tested following ASTM D638 procedure to obtain tensile strength and elastic modulus information of the composites. SEM images of the fracture surface of the specimens after tensile testing, or other suitable technique, were used to evaluate dispersion and to investigate the interfacial adhesion between fibrils and the polymer.

In this subtask, the project team also oversaw development of 3D printable resin systems capable of directly producing new parts or molds that support part production other subtasks. The team conducted experiments to assess printability and final part quality (such mechanical properties, surface properties, rheology, etc.), to remain aligned with the project objective of producing final demonstration recycled composite parts. Parts printed at this stage consisted of mechanical test specimen geometries and small basic shapes (e.g., planks) to assess shape stability.

### 5.5.2. Summary of Experimental Methods

The rGF was cleaned of chars and other residues and sized at Vartega for compounding at SDSMT. The sized rGF was then compounded with neat ABS pellets using a twin-screw extruder and pelletized. The resulting composite pellet feedstock contained 18 wt% rGF and was roughly ~100lbs.

The collected composite pellets were compression molded into bars for characterization along with neat-ABS pellets for comparison. For this purpose, the pellets were loaded into a square mold (length  $\times$  width  $\times$  thickness: 100  $\times$  100  $\times$  1.65 mm), heated at 220 °C for 5 min, and then pressed at approximately 4,536 kg for another 5 min in a Laboratory Press. The pressed plaques were cooled at room temperature under a heavy metal plate (~ 20 kg) for 2 min. After that, the test plaques were cut into multiple slit-shaped bars using a premium guillotine trimmer. The obtained slit-shaped bars were further compression-molded in the Laboratory Press at 220 °C into uniform bars. [8]

The thermal stability of the samples was investigated using a TGA in N<sub>2</sub> at a purge flow rate of 40 mL/min. The dry samples were heated from 25 to 70 °C at a heating rate of 10 °C/min and kept at 70 °C for 5 min to remove the moisture absorbed in the air. Then the samples were heated to 600 °C at a heating rate of 10 °C/min. [8]

The damping (reported as  $\tan \delta$ ) and storage modulus ( $E'$ ) of the samples were determined using DMA. The glass-transition temperatures  $T_g(E')$  and  $T_g(\tan \delta)$  were observed in the onset of the storage modulus drop and the peak of the  $\tan \delta$ , respectively. A multifrequency-strain mode was used, and the strain was 0.05%. A dual cantilever clamp was used on rectangular specimens with dimensions approximately 64  $\times$  9.6  $\times$  2.9 mm<sup>3</sup> (length  $\times$  width  $\times$  thickness). The specimens were tested from 25 to 140 °C at a heat rate of 3 °C/min. [8]

Tensile testing specimens cut both from compression molded bars and 3D printed hexagons were tested on a servo-hydraulic testing machine to determine the tensile strength, Young's modulus, and failure strain, according to ASTM standard D638. The strain rate of 1.524 mm/min and gage length of 12.7 mm were used [8]. Details of 3D printing process are given in section 5.8.

The fracture surface morphology of the tensile tested samples was observed using a Tescan Mira3 SEM. The surface was coated with a sputtering device prior to SEM analysis.

### 5.5.3. Results

Figure 19 shows the TGA curves of neat ABS and rGF/ABS composite. The decomposition temperatures (onset temperature) of both materials were around 403 °C. This indicates that the addition of rGF into ABS did not have a significant effect on the decomposition temperature of ABS. The thermal degradation process for both materials displayed a single step [9]. However, the content of char residues of rGF/ABS composite after the TGA testing was approximately 23 wt%, which was much higher than that of neat ABS (2 wt%). This is mainly due to the rGF left in the char residues after thermal decomposition.

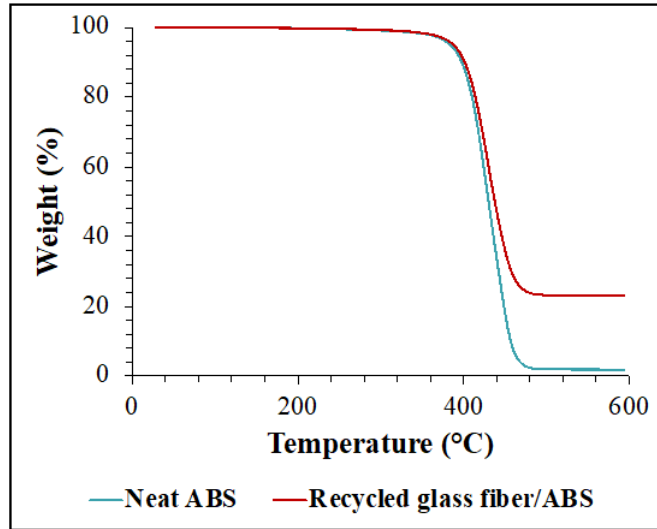


Figure 19. TGA curves of neat ABS and rGF/ABS composite.

Figure 20 shows the temperature dependence of storage moduli and  $\tan \delta$  of neat ABS and rGF/ABS composite. Compared to neat ABS at 40 °C (1479 MPa), the rGF/ABS composite had a much higher storage modulus (2823 MPa), indicating decreased ABS chain mobility in the composite. Compared to neat ABS (2.0), the rGF/ABS composite had a lower  $\tan \delta$  peak (1.5). The lower  $\tan \delta$  peak suggests a restricted segmental chain mobility of ABS molecules, because of rGF during transition at the corresponding temperature [9]. In addition, during the hot-pressing process the rGF/ABS samples exhibited some porosity similar to the rGF/ABS pellets (before hot pressing). These pores are probably due to presence of fiber or other contaminations from the recycling process. After the compression molding process the pores were mainly eliminated to negligible levels.

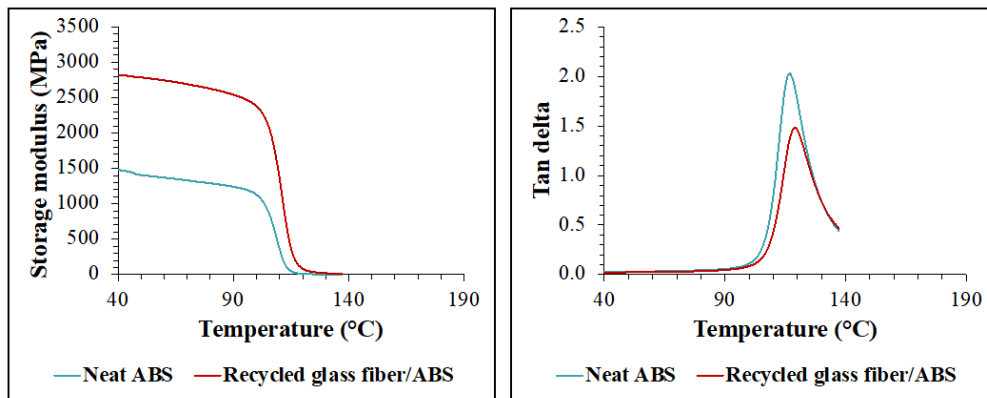


Figure 20. Temperature dependence of storage moduli (left) and  $\tan \delta$  (right) of neat ABS and recycled glass fiber/ABS composite.

Mechanical properties of both compression-molded and 3D printed specimens were measured via tensile testing. The printed specimens were prepared by cutting/machining dog bones both in printing (y) and interlayer (z) directions from a 3D printed hexagon (details of the printing process are provided in Section 5.8). Six samples were machined in each direction following ASTM 638, type 3 specimen dimensions for tensile testing. Table 2 lists the tensile properties of compression molded neat-ABS and rGF/ABS composite, as well as 3D-printed rGF/ABS composites (Y-direction and Z-direction). Compared to neat ABS, the compression-molded rGF/ABS composite showed a 20% higher tensile strength and a 110% higher Young's modulus, proving the reinforcing effect of rGF. As expected, addition of rigid fillers lowered the failure strain compared to neat polymer.

When the tensile properties of the printed samples were investigated, the printing direction samples showed a similar strength to compression-molded rGF/ABS samples, while they are achieving significantly higher modulus. This increase in modulus in the printing direction is an indication of alignment of reinforcing fibers in the testing/printing direction. This also supports the achievement of tensile strength values similar to compression-molded samples. Additive manufacturing process usually results in significantly higher porosity compared to conventional compression molding process, lowering the mechanical properties. However, alignment of reinforcing fibers in the printing direction can compensate some of the property drop due to porosity. Again, as expected, z-direction specimens showed lower strength and modulus values compared to printing direction. While fiber orientation might have an impact in this difference, the main issue arises from weak interlayer adhesion due to nature of the printing process.

Table 2. Comparison of tensile properties for neat ABS, rGF/ABS composite, 3D-printed parts

(Y-direction and Z-direction) (average  $\pm$  standard deviation).

	Tensile strength (MPa)	Young's modulus (MPa)	Failure strain (%)
Neat ABS	35 $\pm$ 1	2062 $\pm$ 34	36 $\pm$ 16
rGF/ABS	42 $\pm$ 6	4323 $\pm$ 498	3.8 $\pm$ 0.5
3D-printed part (Y-direction)	40 $\pm$ 1	5428 $\pm$ 190	2.9 $\pm$ 0.3
3D-printed part (Z-direction)	18 $\pm$ 1	2307 $\pm$ 72	3.7 $\pm$ 0.9

Figure 21 shows the fracture surfaces of compression-molded neat ABS and rGF/ABS composite after tensile testing. While neat ABS exhibited a relatively smooth fracture surface, rGF/ABS composites had a much more porous surface. These voids basically suggest fiber pullout from the fiber-matrix interface failure during tensile testing [8]. The clear fiber surfaces observed in the SEM images suggest a poor fiber-matrix interfacial adhesion, despite the application of a sizing. Application of surface treatments or more compatible sizing might increase the fiber-matrix interfacial adhesion leading to further improved mechanical performance.

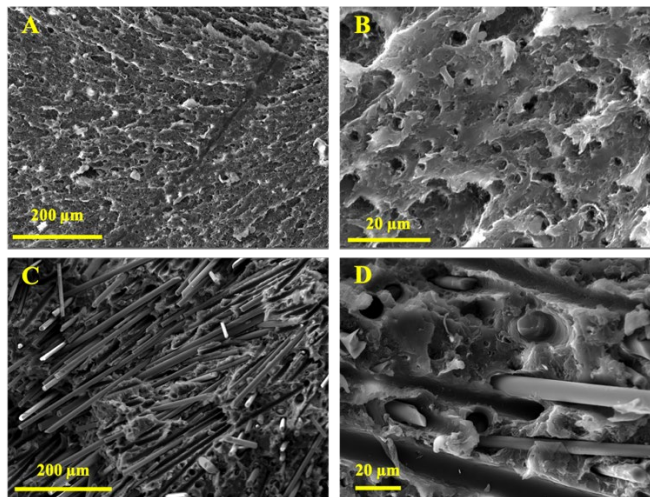


Figure 21. SEM images of fracture surfaces of neat ABS (A and B) and rGF/ABS composite (C and D) at two different scales of 200  $\mu$ m and 20  $\mu$ m.

## 5.6. Expanded TEA and LCA of rGF and rCF

### 5.6.1. Scope

A successful business case for composite recycling will require a cost below \$100/ton to provide recovered product and an attractive investment payback of 2 years or less. This would allow a competitive cost with solid waste landfill disposal, where the average US landfill tipping fees (\$55.63/ton in 2019) and freight cost (\$15-60/ton) will allow a reasonable above ground storage regional model for recycling as an end-of-life solution. Municipal solid waste (MSW) landfill tipping fees in the U.S. continue to rise, with fees increasing from 2018 to 2019 by \$2.74, or 5.2 percent, according to new research from the Environmental Research & Education Foundation (EREF). The EREF Data & Policy Program's recently released 2019 Landfill Tip Fee Data report found that the national average MSW tip fee is now \$55.36 per ton. This is based on waste hauled in dumpster truck or reefer in 2021 relative to state compliance and within 200 mile radius, based on \$30-\$60/ton freight cost.[10,11,12]

Examples from the LCA are given to reduce carbon impact and achieve financials by selling into sheet molding compound (SMC), BMC, 3D printable, or engineered thermoplastic applications and/or through shared Thermolyzer™ investment with other industries like tires or consumer plastics. The subtask work focused on developing an expanded TEA to benchmark and prepare the business case for utilizing mechanical shredding/grinding and controlled pyrolysis technology for composite material recycling. Pyrolysis processing data, recovered fiber quality results, and LCA from Project 6.4, the pre-task work and Subtask 6.29.2, were combined to provide the carbon impact and potential economics of controlled pyrolysis fiber recovery. The relative value for each potential market was compared through price sensitivity and elasticity. The business case considered the shipping and handling cost and the commercial value of filler and fiber blends and residual materials.

### 5.6.2. Summary of Experimental Methods

The TEA/LCA model makes the following assumptions:

- 1. Conservative Case.** The LCA of controlled pyrolysis recycling assumes the inherent energy in composites of over 15% resin weight content is used to fuel the process, and it preserves substantial mechanical property value in the rGF and rCF for reuse. The TEA is conservative for the full investment case and does not account for recycling other waste streams at the same facility to spread capital risk across multiple industries for economy of scale. Instead, a shared investment case is given for comparison.
- 2. Circularity.** Circularity in terms of cradle-to-cradle sustainability assumes the composite raw materials remains in use indefinitely by cascading within the composite part application, within industry (eg. transportation, infrastructure), and within the greater composite industry until sequestered to reduce carbon impact.
- 3. Regional Model.** High-volume composites impose significant waste handling costs at end-of-life and require a regional model with maximum 500-mile radius for trucking or several thousand miles for barge delivery.
- 4. Critical Fiber Length.** Recovered fiber meets specifications for critical fiber length after composite part fabrication for wind, industrial or automotive parts using 3D printable, BMC, or thermoplastic compounding extrusion with compression or injection molding to meet light-weighting requirements supporting circularity and substitution of traditional materials. This also assumes the baseline mechanical properties and processing capability of chopped fiber composite preforms meet composite part requirements.

5. **Required Robustness.** The four different waste streams that were evaluated represent the robustness required:
  - Wind blade rGF and rCF for 3D printing of test coupons and components.
  - Semi-trailer panels with rGF in extrusion compression molding of PP flat panels with various levels of GF loading 30% to 50% by weight.
  - Forward lighting BMC components in automotive using up to 25% by weight rGF.
  - Tractor door part using 10-20% rGF in thermoplastic diaphragm molding HDPE/PP.
  
6. **Value of rGF.** The value of rGF falls within the range used for the application sensitivity analysis of 0.40, 0.60, 0.80, 1.60, and 2.40 \$/kg. This reflects the potential range of market values in the different applications identified and evaluated (Table 3), while also accounting for the performance of the recycled versus the competing “on-purpose” alternatives. The lower \$/kg values represent recycled product with higher variability of fiber length for the recovered fiber with value in commoditized segments (e.g., BMC, or high density polyethylene (HDPE) and/or polypropylene (PP) compounds), whereas higher \$/kg values represent applications using engineering thermoplastic resins (e.g., Polyamide, polybutylene terephthalate (PBT), polycarbonate (PC)/ABS).
  
7. **Other Key Assumptions.** Other key assumptions for the TEA included the following:
  - Range of delivered cost for composite end of life (EOL)/Scrap is \$0 to \$200/ton, where \$0/ton assumes that the EOL/Scrap generator incurred the full cost to ship like Landfill. The cost incurred by Thermolyzer™ facility for freight and handling assumes potential for higher transportation/fuel costs and additional handling fee at EOL/Scrap storage facility.
  - Mass/Energy Balance – EOL Spar Cap (Table 3 - Case 1) and Shell/Root Section (Table 3 - Case 4) based on CHZ pilot scale testing of sampled composite EOL/Scrap stream.

Table 3. Mass/Energy Balance from Project 6.4 using CHZ Pilot line to process commercially supplied composite EOL/Scrap (Cases 1 to 4)

Composite Recycle (scrap) Stream (RM - Raw material)	Est. RM Feed Split	Mass Balance		Energy Balance (MJ basis)		
		FP Yield	Waste (solid/liquid)	TE	EC	NE
		kg RM/kg FP	kg Waste/kg FP	MJ/kg FP		
1 CF epoxy wind blade spar cap GE (70% solid content)	5%	1.43	0.010	3.93	(3.93)	-
2 GF/CF epoxy hybrid John Deere (70% solids content)	5%	1.43	0.010	3.93	(3.93)	-
3 GF polyester/ vinyl ester automotive CSP (60% solid content)	45%	1.67	0.010	3.37	(4.72)	(1.35)
4 GF epoxy balsa/PVC foam wind blade GE (50% solid content)	45%	2.00	0.010	2.81	(5.61)	(2.81)
<b>Total Combined Stream (per unit of FP, or recovered Fiber)</b>	<b>100%</b>	<b>1.79</b>	<b>0.010</b>	<b>3.17</b>	<b>(5.04)</b>	<b>(1.87)</b>
<b>Total Combined Stream (per unit of RM, or composite scrap)</b>			<b>0.006</b>	<b>1.77</b>	<b>(2.81)</b>	<b>(1.04)</b>

FP - Finished Product (i.e., recovered Fibers from Thermolyzer)  
 RM - Raw Material (Shredded Recycle Composite fed to Thermolyzer)  
 TE - Total Energy to Convert RM to FP  
 EC - Energy Credit from organics - Recoverable Energy  
 NE - Net Energy - Zero/Negative - Energy neutral/Net energy producer

- CAPEX - Assumes CHZ investment cost estimate of \$58mm for 120 kilotons per annum (kta) Raw Material (RM) Composite EOL/Scrap facility
- The Capacity on a Recovered fiber Finished Product (FP) basis is a function of the fiber content, and the Mass Balance (recovered fiber of RM input) from the CHZ Pilot work. Thus, the Finished Product (FP) capacity for the two EOL/Scrap streams evaluated are as follows:

- Case 1 (EOL Spar Cap): FP Capacity = 84 kta)
- Case 4 (EOL Shell Section): FP Capacity = 60 kta
- Sales Volume - 57 kta sales volume after year 5 for both Case 1 (67% utilization) and Case 4 (95% utilization). Used same sales volume to compare the two cases, and assessed the impact of RM feed.

### 5.6.3. Results

Tables 4A and 4B show the financial summary for the full investment case of \$58mm using different EOL/Scrap (A – Spar Cap, B – Shell Section) as the RM inputs. Since the sales volumes were held constant at 57 thousand tons per annum (kta), for RM cost of \$50/ton RM or higher, feeding the higher fiber content EOL Spar Cap Scrap is advantaged, as more of the RM is converted to FP. For example, at \$50/ton RM cost, the FP cost will vary by EOL/Scrap type (i.e., fiber content) as follows

- Case 1 (Spar Cap) = \$72/ton FP (\$50/ton RM \* 1.43 kg RM/kg FP)
- Case 2 (Shell Section) = \$100/ton FP (\$50/ton RM \* 2.0 kg RM/kg FP)

Even though the higher organic/resin (and BTU) content contained in the Shell (~50%) vs Spar Cap (~30%) EOL/scrap would yield greater benefit in terms of excess recovered energy (Syngas that could be sold to an electrical utility), this would only provide a financial advantage to the Shell EOL/Scrap feed at an RM cost of \$0/ton (see Table 4A and 4B). However, at virtually all RM costs above \$0/ton, the higher glass content in the Spar Cap (70% vs the 50% in the Shell EOL/Scrap) would have a much greater positive impact on the FP cost (and therefore the overall financial attractiveness) than the negative effect of the lower organic/resin (and BTU) content vs the Shell EOL/Scrap.

In addition, the higher glass content in the Spar Cap EOL/Scrap RM feedstock would yield higher recovered sellable fibers (Finished Product/FP) resulting in more efficient use of the \$58.5mm CAPEX. Thus, with the Spar Cap EOL/Scrap feedstock, the total sellable FP is ~84 kta (120 kta RM/1.43), while the total FP that can be produced with the Shell Section EOL/Scrap is only ~60 kta (120 kta RM/2.0). Clearly, having a feedstock with higher glass content would yield higher revenues and higher NPV, resulting in higher capital efficiency (NPV/investment).

Table 4. Financial summary of the full investment case of \$58.5mm CAPEX at different RM costs and FP Values

<b>Table 4A – EOL/Scrap Spar Cap (~ 70% Glass)</b> RM/FP Capacity – 120 kta/84 kta Sales (year 5): 57 kta (67% Utilization)							<b>Table 4B – EOL/Scrap Shell (~50% Glass)</b> RM/FP Capacity – 120 kta/60 kta Sales (year 5): 57 kta (95% Utilization)						
RM Cost	GF Price	Financial Summary (CAPEX = \$57.5 mm)					RM Cost	GF Price	Financial Summary (CAPEX = \$57.5 mm)				
\$/ton	\$/ton	NPV6 (\$mm)	CF 5YRS (\$mm/yr)	XIRR (%)	Payback (YRS)	ROCC (%)	\$/ton	\$/ton	NPV6 (\$mm)	CF 5YRS (\$mm/yr)	XIRR (%)	Payback (YRS)	ROCC (%)
0	400	33	16	19%	N/A	9%	0	400	35	16	20%	N/A	9%
	600	81	23	34%	4.1	21%		600	82	24	34%	4.1	21%
	800	128	31	46%	3.5	32%		800	130	31	46%	3.4	32%
	1,600	319	61	84%	2.2	72%		1,600	320	62	84%	2.2	73%
	2,400	509	92	116%	1.7	107%		2,400	511	92	117%	1.7	107%
50	400	15	13	13%	N/A	4%	50	400	9	12	10%	N/A	3%
	600	63	21	29%	4.5	16%		600	57	20	27%	4.6	15%
	800	110	28	42%	3.7	28%		800	105	27	40%	3.8	26%
	1,600	301	58	80%	2.3	68%		1,600	295	58	79%	2.3	67%
	2,400	491	89	113%	1.7	103%		2,400	486	88	112%	1.7	102%
100	400	(3)	10	4%	N/A	-1%	100	400	(16)	8	-3%	N/A	-5%
	600	44	18	23%	4.9	12%		600	32	16	19%	N/A	8%
	800	92	25	37%	4.0	23%		800	79	23	34%	4.2	20%
	1,600	282	55	77%	2.4	64%		1,600	270	53	75%	2.4	61%
	2,400	473	86	110%	1.8	99%		2,400	460	84	108%	1.8	97%
150	400	(21)	7	-6%	N/A	-6%	150	400	(41)	4	-25%	N/A	-13%
	600	26	15	17%	N/A	7%		600	6	11	9%	N/A	2%
	800	74	22	32%	4.3	19%		800	54	19	26%	4.7	14%
	1,600	264	53	74%	2.5	60%		1,600	244	49	70%	2.6	56%
	2,400	455	83	107%	1.8	96%		2,400	435	80	104%	1.9	91%
200	400	(39)	4	-23%	N/A	-13%	200	400	(67)	(0)	n/m	N/A	-22%
	600	8	12	10%	N/A	2%		600	(19)	7	-4%	N/A	-5%
	800	56	19	27%	4.6	14%		800	29	15	18%	N/A	8%
	1,600	246	50	70%	2.6	56%		1,600	219	45	65%	2.7	50%
	2,400	437	80	104%	1.9	92%		2,400	409	76	99%	2.0	86%

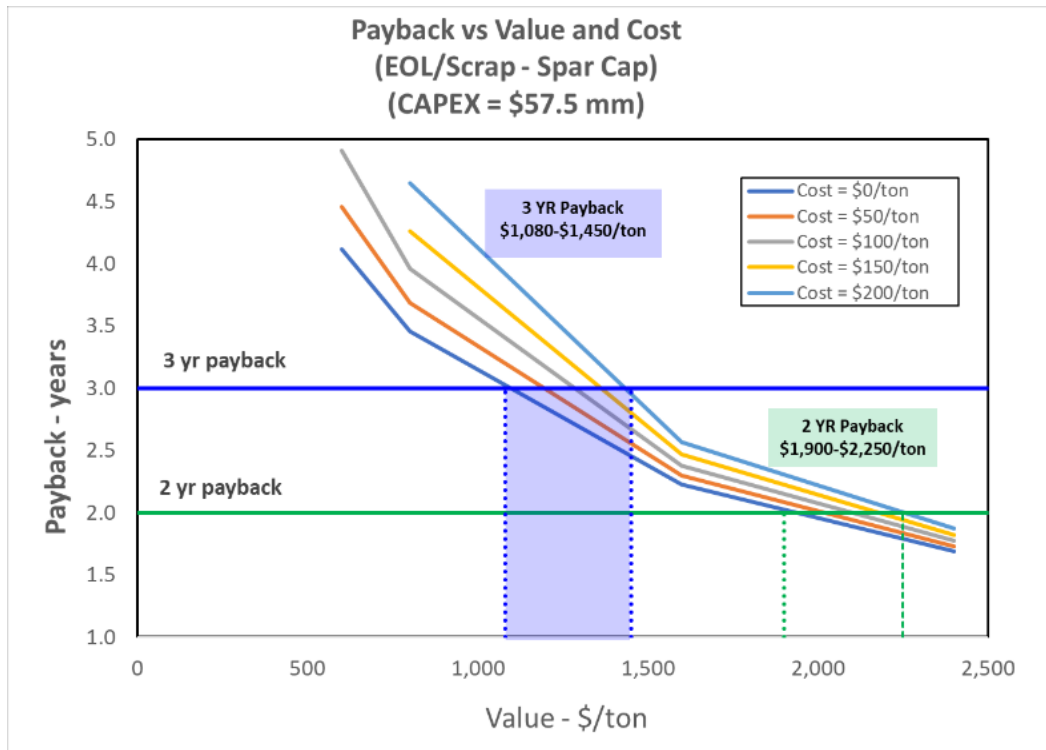
o RM – Raw Material (Composite EOL/Scrap)  
 o FP – Finished Product (Recovered Fiber)  
 o Financials – 5 Year Cash Flow (CF) with 5X Terminal value (assumed 5X last 2 years of EBIT)  
 o NPV6 – Net Present Values with 6% discount rate  
 o CF – Cash Flow (after year 5); ROCC – Return on Capital Consumes (5 Year average)

The estimated range of FP values that would be required to achieve a 3 and 2-year payback (with the Spar Cap EOL/Scrap feedstock), at the different RM Costs (\$0 to \$200/ton) for the full investment case are as follows (see Table 5):

- 3-year payback: \$1,180/ton (at 100/ton RM Cost) with Range of \$1,080 to \$1,450/ton
- 2-year payback: \$2,010/ton (at 100/ton RM Cost) with Range of \$1,900 to \$2,250/ton

To attract investment, in addition to favorable Net Present Value (NPV), Internal Rate of Return (IRR) and Return on Corporate Capital (ROCC), having 2-year or less payback time is highly desirable. However, the above FP values that are required to achieve these returns are generally higher than the virgin chopped glass alternatives (\$800 to \$1,000/ton range). Thus, target applications must have sufficient value for Post-Consumer Recycled (PCR) fiber to justify the premium pricing above the virgin alternatives. For example, higher premium could be justified if the PCR fiber enables buyer to drive incremental top-line (i.e., volume and revenue) growth in end use applications requiring recycle content driven by sustainability with lower carbon footprint in a circular economy that would not be achieved with the virgin alternatives.

Table 5. Payback vs value at different cost levels for full investment case (\$58.5mm)



However, if the PCR fiber values are not attainable, another option to achieve favorable financials with the desired 2-year payback is to reduce Capital Expenditure (CAPEX). A potential strategy to reduce CAPEX is to leverage an existing facility or share in the investment of a new Thermolyzer™ asset between industries such as consumer plastic or tire recycling. At higher capacity the capital intensity (CI = \$investment/kg FP) will be lower, which will improve investment economics with faster payback. Of course, the higher capacity asset will also require higher sales volumes (but not as high price as would be necessary for the lower capacity higher CI investment). Note, different investment/capacity (i.e., CI) levels were considered in Phase I [1] of this project. Table 6 shows the CAPEX and CI at various RM capacities, assuming a scrap glass content of 50% (from Table 4B EOL/Scrap Shell).

Table 6. CAPEX and CI at Various RM Capacities

RM Capacity (kta)	FP Capacity Equivalent (kta)	CAPEX (\$mm)	CI
120	60	57.5	0.96
60	30	31.9	1.06
30	15	18.2	2.43

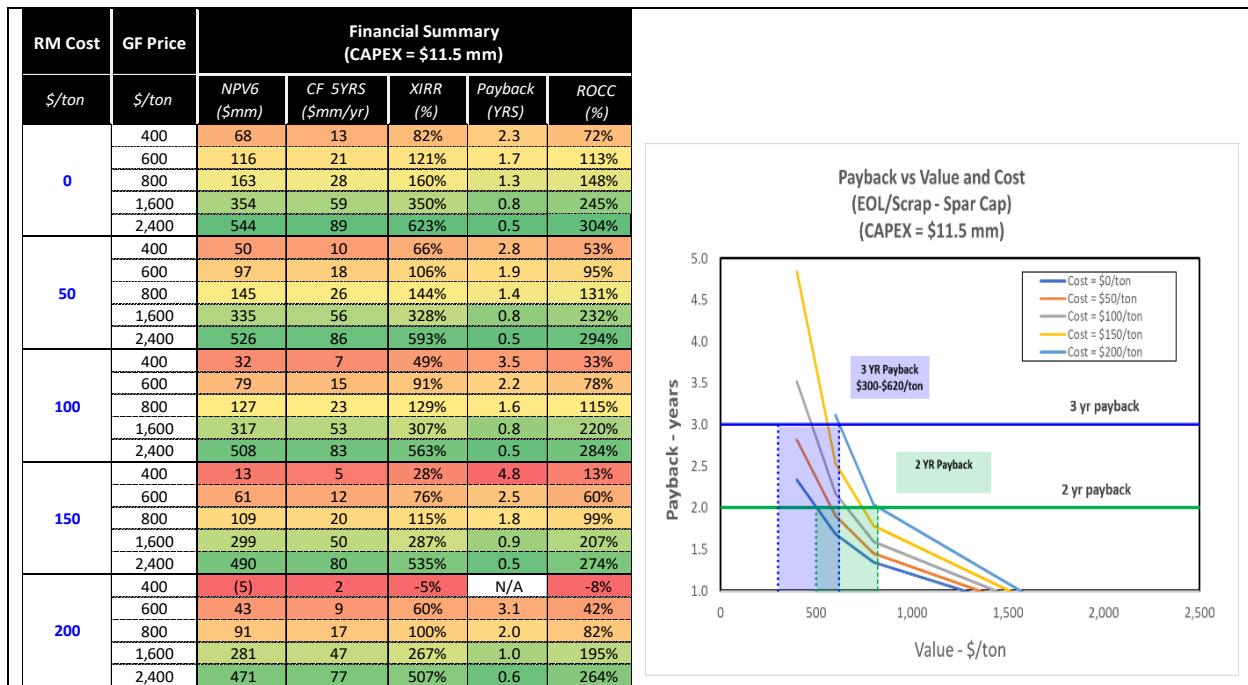
Leveraging an existing facility also would require incremental investment to handle and process the additional EOL/Scrap from composites (i.e., RM storage, feed to Thermolyzer™, composite waste handling, FP fiber storage/handling, and other ancillary equipment), versus a full “Greenfield” where the investment in a new Thermolyzer™ asset would share the CAPEX burden with the processing of other non-composite EOL/Scrap feedstocks. For a full “Greenfield”, further investment (and processing cost: e.g., transitional storage tanks, solvent extraction, etc.) would be required for any necessary process equipment (and additional processing) to mitigate the impact of such contaminants to yield a sellable recovered rGF or rCF product.

Table 7 shows the financial summary for a **shared investment case**, assuming an \$11.5 mm investment (i.e., 20% of full investment) with Spar Cap EOL/Scrap, and the same 57 kta year 5 sales volumes used for the full investment cases above. Table 8 shows the estimates for the range of FP values required to achieve a 3 and 2-year payback at a range of RM cost of \$0 to \$200/ton for the shared investment case:

- 3-year payback: \$460/ton (at 100/ton RM Cost) with Range of \$300 to \$620/ton
- 2-year payback: \$650/ton (at 100/ton RM Cost) with Range of \$500 to \$820/ton

Table 7 (left). Financial summary for shared investment case (~20% of full CAPEX = \$11.5 mm) at different RM costs and FP Values

Table 8 (right). Payback vs value at different cost levels for shared investment (20% of full CAPEX = \$11.5mm) case



In summary, to achieve an attractive return in a full investment case would require targeting the applications with strong sustainability drivers or premiums that can justify the higher value for PCR fiber versus the competing virgin fiber alternatives. Although several applications were identified and evaluated that could provide some demand pull-through, the opportunity for value above virgin fiber may limit the volume and growth potential (i.e., price-volume elasticity), unless there is for example a 10% premium per 10% increase in PCR content. To drive adoption and create higher volume pull-through would require positioning PCR at or below the virgin fiber value. Then, however, to achieve attractive financials would require lower investment costs. This could be accomplished by leveraging existing Thermolyzer™ assets and/or sharing the investment with other industries.

The LCA and economic impact of pyrolysis recycled fiber with the Thermolyzer™ could be a viable part of the cascade of composite raw material life for the circular economy. Remanufacturing the composite part might well be the first step for cascading within the composite part application, and then recycled for recovery of fiber with the Thermolyzer™ within industry and cascading until sequestered to reduce carbon impact for cradle-to-cradle sustainability.

## 5.7. Recycled Composite Demonstration Part Fabrication—Part A: Automotive Vehicle Part Molding Trials

### 5.7.1. Scope

In this subtask, preforms developed in Subtasks 6.29.3 were used to mold example automotive parts. Processing conditions were established for appropriate molding procedures, such as injection or compression molding, to yield final demonstration parts. The lightweighting potential of the produced recycled composite part was compared against traditional materials used. Based on the earlier comparison of recycled composite performance versus existing industry product and application needs from Subtask 6.29.3, the project team decided to pursue a few additional target applications of opportunity, subject to approval by the wider project team provided sufficient recycled fiber was available.

OEMs realize energy (light weighting) and cost (use of recycled materials) benefits by replacing metallic parts such as aluminum, magnesium with composites solutions. In this work two representative parts were considered to demonstrate recycled composites in automotive vehicle applications. These include: (a) seat back rest and (b) battery tray cover. Both of these are representative part geometries meant to evaluate the materials-processability and properties. The parts were not specific to a vehicle model or manufacturer. The seat back rest was evaluated for a range of materials including traditional glass/vinyl ester SMC, SMC with continuous tape over molding, wood stock PP, flax and recycled CF mats. For purposes of this report, we illustrate the recycled CF mats for evaluating processability into the seat back rest.

The battery tray tool part was processed via fiber-polymer injection molding and extrusion-compression molding. This part was evaluated for several virgin materials and recycled materials. For purposes of this report, we report the recycled material in producing the battery tray tool part.

A John Deere door panel part was processed via vacuum thermoforming of laminated DiFTS materials [6,7] using Thermolyzer<sup>TM</sup>-recovered carbon and glass fibers in HDPE and HDPE/PP polymer matrices.

### 5.7.2. Summary of Experimental Methods

#### Seat back rest

A two-cavity aluminum seat back rest tool was used in this work to evaluate the scale up manufacturing. The computer aided design (CAD) concept for the core and cavity of the tool is shown in Figure 22. The tool is nominally 76 cm × 45.7 cm × 35.6 cm with features including steps, bends and curvatures. This enables the evaluation of different materials for processability into different shapes and features.

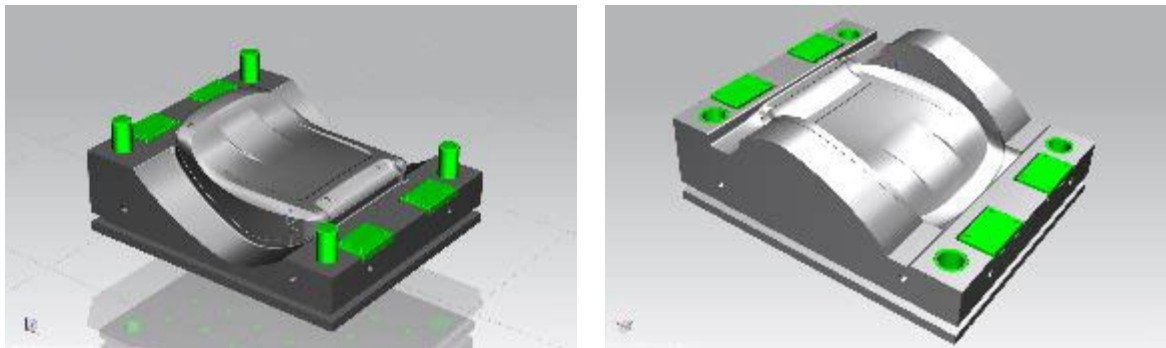


Figure 22. CAD rendering of the seat back rest tool cavity (left) and core (right). The tool is approximately 76 cm × 45.7 cm × 35.6 cm and weighs ≈ 910 kg.

The material was 30wt% rCF/PA66 random chopped mats from Carbon Conversion Solutions (CCS) for these trials. Figure 23 illustrates the processing sequence. Three layers of the rCF mats were cut to the part dimensions with about 2” clearance for each side to fold over. The sheets were stacked and subjected to a ProTherm™ conveying infrared heater 4ft wide, 8ft long and 1ft clearing height. The rCF-PA66 mats were passed on to the conveying mesh belt of the oven. The stack was dwelled for 3 min at 600F until a slight amount of smoke was observed – indicative of the PA66 having attained its sag (processing temperature). The stack was picked up manually at the exit end of the oven and quickly transferred to the tool (mounted in the press) as shown in Figure 23. The mold was subjected to 1900 kN and a 5-minute cycle time was used. The tool temperature was approximately 350F maintained through oil heating. The part consolidation was acceptable as evident from the demolding as shown.



Figure 23. Processing sequence of infrared (IR) heating of the rCF-PA66 mat and transfer to the press for compression molding. Left to right: IR heating of rCF-PA66 in conveying oven; transfer heated rCF-PA66 to press (tool); 5-min cycle time and demold; and back side of the part.

The recycled material works best in contact heating, i.e., during the contact with the mold. Ideally this part can be produced with a higher tool temperature (about 500F), however we were limited in the configuration of the mold to attain 500F. There is some loss of heat during transferring the sheet from the IR oven to the tool and closing of the tool. Albeit this is less than 20 seconds in total, the surface area of the recycled CF-PA66 mat is large and can begin to lose heat rapidly. These issues can be readily addressed in production through heat blankets and in-line transfer of the heated mat directly to the press avoiding the manual step of transfer.

### **Battery tray part**

In the current work, a representative battery tray cover abbreviated as ‘BT’ tool was used to study property bounds of discontinuous fiber composites produced via multiple processes including injection molding (IM), injection compression molding (ICM) and extrusion-compression molding (ECM). The BT tool design was conceived to be agile for use in multiple processes, i.e., IM, ICM and ECM. The material forms include compounded pellets, long fiber thermoplastics (LFT) and rCF-PA66 and rCF-epoxy materials. The BT tool design allows for the manufacture of components with the most efficient process or materials, without building multiple single process tools. The data generated by this study provides a baseline for the development of components, materials, and processing options without having to invest in multiple tools.

For the recycled material, two processes were used- (a) IM of compounded recycled carbon fiber (rCF/PA66 compounded pellets), and (b) rCF-epoxy charge (like bulk molding compound) which was compression molded using *the same* BT tool. The results from these were compared against a range of other processes not included in this study.

A 400 ton Van Dorn Injection Mold Press with 60oz shot size was used in producing the battery tray cover parts based on the recycled materials. Representative short shots shown in Figure 22a illustrate the flow/fill of the recycled charge. During short shot runs there is some degree of non-uniformity in the fill as the process was being optimized. The corners are the last to fill. The thin ribs did not fill in the initial attempts.

### **John Deere Door panel**

A high molecular weight, high density polyethylene (HDPE) regrind, used in many John Deere parts, was the base matrix resin in this study, to which polypropylene (PP) was added as a viscosity modifier to enhance processibility, resulting in an 80:20 HDPE:PP blend.

The rCF and rGF were cyclone-cleaned (see Figure 16). The rCFs were aggregated and sized by Vartega and fed to the DiFITS process through the extruder hopper. Due to resource limitations, the rGF was not aggregated and sized, but was hand-fed to the extruder at prescribed time intervals. A hybrid combination of the rGF and rCF was also fed to the extruder in one of the trials, since mixed GF/CF feedstocks are recoverable from John Deere spray booms, and this mixed material is therefore of particular interest to the company.

Limited availability of the rCF and rGF for this part of the project meant that fiber loading levels were kept to 10wt%. Fiber reinforced sheets were produced by the DiFITS process. For each fiber type, some of the sheets were laminated and cut into test coupons for mechanical property evaluation. Some of the sheets containing the carbon/glass fiber mixture were laminated into ~6mm thick, 4' x 4' panels for molding trials.

A (male) tool for a John Deere door panel was used for the vacuum thermoforming process, which was carried out by a John Deere contractor using the thermoforming machine shown in Figure 24. Temperature and vacuum pressure were studied to determine optimum conditions for forming the hybrid CF/GF composites.



*Figure 24. Vacuum thermoforming machine and tool used to mold the John Deere door panel.*

### 5.7.3. Results

#### **Seat back rest**

The nominal part thickness was measured at 15 locations and was confirmed to be 2.8 mm +/- 0.15 mm. In the current part (where the tool had limitations of heating to 500F) a post-step of thermoset infusion can be done to obtain a high stiffness part. An example of glass fiber structural SMC is shown in Figure 25 with the note that rGF can be converted to a bulk charge and molded like an SMC. There are multiple options to develop recycled products through these approaches. Post evaluation of the seat back rests were conducted through flexure, interlaminar shear and vibration damping evaluation.

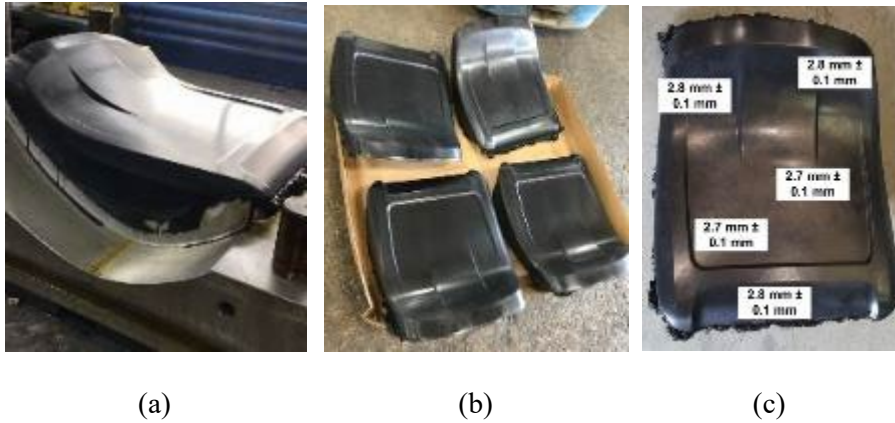


Figure 25. SMC seat back rest seats: (a) the charge placement was optimized for cycle time 3 minutes with no visible defects; (b) the flash is marginal, which can be eliminated in production with a sharper shear edge; and (c) thickness profile of the seat back was consistent. Future parts can use rGF-vinyl ester bulk charge and mold in a similar fashion.

### Battery Tray Part

Figure 26 illustrates the sprues from different part runs. With several trial-and-error runs, the process was optimized to achieve full fill as shown in Figure 26b, with the sprue still attached. A high degree of preferential orientation was noted in the sprue. The definition of the ribs on the underside was excellent. No print through was observed once the process was optimized.



Figure 26. Representative battery tray cover parts made from rCF-PA66 and rCF-epoxy. The parts look very similar for both materials. (a) short shot in IM of rCF-PA66 and (b) fully filled part.

A range of mechanical testing included flexural strength & modulus, interlaminar shear, and Izod impact to compare the rCF variants to other materials. Table 9 summarizes some of the variants comparing to rCF processed in this study. It can be seen that despite the starting material variants, the properties of the rCF are compatible to virgin and textile grade CF-based intermediates.

Table 9. Preliminary mechanical test data of rCF thermoplastics and thermosets compared to long fiber virgin and textile grade carbon fiber thermoplastics

Material	rCF-PA66 (30 wt%)		rCF-epoxy (30 wt%)		LFT C-PA66 <sup>1</sup> (50 wt%)		TCF-C-PA66 <sup>2</sup> (30 wt%)	
	½” starting fiber length - Compounded pellets		Bulk charge, ½” fiber length		½” fiber length, hot melt impregnated pellets		½” starting length, compounded pellets	
Flow direction	Along <sup>3</sup>	Across <sup>4</sup>	Along	Across	Along	Across	Along	Across
Flexural strength (MPa)	206	86	514	113	202	103	115	55
Flexural modulus (GPa)	19	7	23	12	14	4	17	4
Interlaminar strength (MPa)	29	17	16	16	34	23	16	12
Izod impact strength	19	12	18	13	27	15	18	6

<sup>1</sup>LFT C-PA66 is Complete long fiber ½” fiber length pellets, 50 wt% fiber fraction.

<sup>2</sup>Textile grade carbon fiber compounded pellets, the TCF is produced at Carbon Fiber Technology Facility at ORNL.

<sup>3</sup>Fibers align preferentially along the flow direction (Along).

<sup>4</sup>Across is transverse to the flow direction.

### John Deere Door Panel

Table 10 shows the tensile strength and modulus properties of the composites produced using the HDPE and the HDPE/PP blends as matrix resins. Whereas the Thermolyzer<sup>TM</sup>-recovered carbon fiber provided a useful level of reinforcement, even at only 10 wt% addition, the rGF showed a very weak or negligible reinforcement effect at this fiber loading. The rCF/rGF combination showed a significant increase in tensile modulus at a 10 wt% fiber loading, but there was no significant influence on tensile strength. We believe that the lack of influence of the GF reinforcement arises from the absence of sizing and the low loading level (which could not be increased above 10 wt%, due to limited availability of the rGF).

Table 10. Mechanical properties of the HDPE and HDPE/PP composites reinforced with rGF, rCF and rGF/rCF mixture.

Polymer	Type of thermolyzer-recycled fiber	Fiber loading level	Laminate strength (MPa)	Laminate modulus (GPa)
HDPE	None	0	23	1.2
HDPE	Carbon	10%	41	5.6
80%HDPE/20%PP	None	0	25	1.5
80%HDPE/20%PP	Carbon	10%	43	6.1
80%HDPE/20%PP	Glass	10%	23	1.8
80%HDPE/20%PP	Carbon/glass hybrid	5% carbon 5% glass	26	2.4

After several temperature/pressure optimization runs, the laminated panels containing the rCF/rGF mixture were successfully vacuum thermoformed into the door panel, and 6 replicate parts were produced, as seen in Figure 27. It may be noted that vacuum thermoforming is a fast and low-cost method of part production, and hence highly suited to applications using low-cost recycled fiber feedstock.

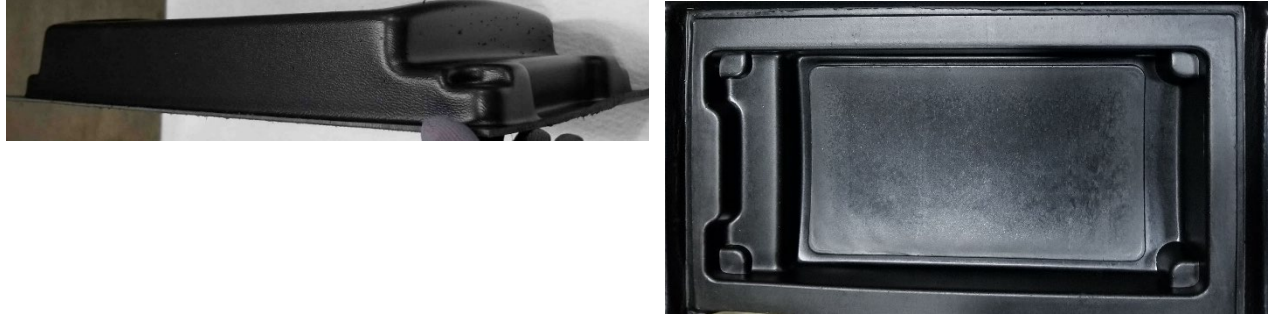


Figure 27. Vacuum thermoformed door panel part, molded from a rCF/rGF mixture in an 80:20 HDPE/PP matrix. (The HDPE was a recycled polymer).

## 5.8. Recycled Composite Demonstration Part Fabrication—Part B: BAAM Composite Development and Test Part Analyses

### 5.8.1. Scope

In this subtask, composite resin systems were developed and optimized for BAAM production. Thermoplastic compounded composites from Subtask 6.29.3 were pelletized and optimized for extrusion. Resin composition for recycled fiber blends were analyzed via rheological instruments to ensure consistent resin flow and extruded melt strength. Additives and fiber surface chemistry were adjusted as necessary to achieve appropriate extrusion performance. BAAM printed parts were assessed for fiber distribution and potential alignment through measurements such as part warping and x-ray chromatography scans. The mechanical performance of the printable resins developed in Subtask 6.29.3 was presented to the ORNL-MDF team to discuss options for printing large-scale parts using rCF and rGF.

### 5.8.2. Summary of Experimental Methods

The complex viscosities and storage moduli of the samples were studied using a Discovery hybrid rheometer (TA Instruments) within the linear viscoelastic region at 220 °C. The gap was set at 500  $\mu\text{m}$ . Parallel plates (aluminum disposable) with 8 mm diameter were used for the frequency sweep tests (from 0.1 to 100 rad/s) [8].

A hexagon with 10” side dimensions and a 10” height was first printed using a BAAM system by Cincinnati Inc. for characterization. The feedstock pellets were dried for 6 hours at 145F prior to printing. A 0.3” nozzle along with a 0.15” layer height and a 0.34” bead width was used. The extruder temperature profile was set to 176, 176, 230, 230, 235°C and roughly a 1.5 min layer time was used. Tensile testing specimens in both printing and interlayer direction (z-direction) and x-ray computed tomography (CT) specimens in printing direction were cut/machined from the printed hexagon.

The X-ray CT scan of the specimens cut from the 3D-printed part was performed using a Zeiss Xradia Versa 520 equipment. The high-resolution scan used a 40 kV x-ray energy with a 1.25  $\mu\text{m}$  voxel size whereas the low magnification scan was performed at 60 kV with an 18.17  $\mu\text{m}$  voxel size. Data visualization and analyses were performed using the DragonFly PRO software.

Once the characterization of the printed sample part (hexagon) was completed, the remaining rGF/polymer feedstock material was used to demonstrate additive manufacturing of a section of a submersible device designed by Dive Tech and ORNL.

### 5.8.3. Results

One of the critical parameters for extrusion based additive manufacturing process is the feedstock material melt rheology at process temperatures and different shear rates. Figure 28 shows the change in complex viscosity as a function of the angular frequency of neat ABS and rGF/ABS composite at 220 °C, at which the compression molded samples were prepared. As expected, the presence of reinforcing fibers led to an increase in viscosity of neat polymer. Similarly, the addition of rGFs also increased the storage modulus of the polymer significantly. The complex viscosities of both neat ABS and rGF/ABS composite showed a shear-thinning behavior, i.e., they decreased as the angular frequency increased [9]. High viscosity at zero shear (i.e., zero angular frequency) is desirable for large-scale 3D printing, as the extruded composite has to retain its shape after deposition. The decrease in complex viscosity with angular frequency is also favorable for large-scale 3D printing, as it reduces the torque and energy requirements during the 3D printing process [8].

During the printing process optimization, initially the extruded beads shark skinned at the standard temperature profile used for printing CF-ABS feedstock material (i.e., 176,176,249,249,249 °C) and the extrudate viscosity was observed to be too low at these temperatures and did not form a solid bead to build on. Therefore, the temperature profile was reduced down to 176,176,230,230,235 °C. The torque measurement at 50 rpm extrusion speed was 55% and 80% at 200 rpm. Initially some oozing occurred during lifts for start and stops at each layer, which led to poor start and stop quality; however, bead quality improved after the first 4-5 layers during printing the hexagon.

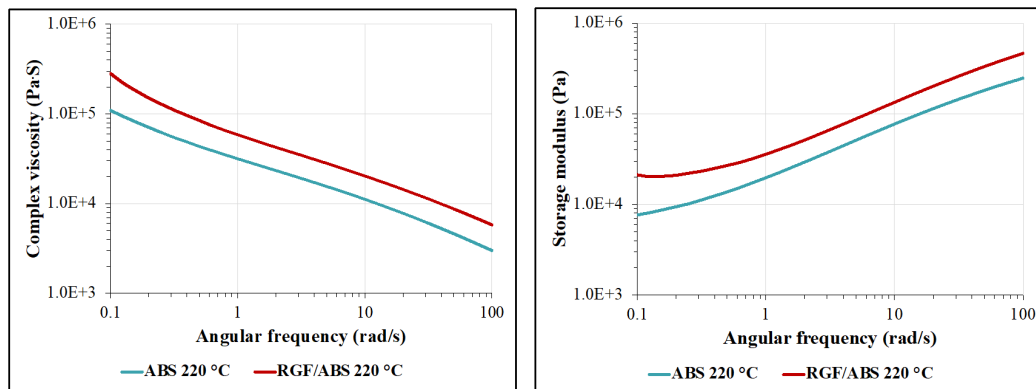


Figure 28. Left: Change in complex viscosity as a function of the angular frequency of neat ABS and rGF/ABS composite (rGF/ABS) at 220 °C. Right: Change in storage modulus as a function of the angular frequency of neat ABS and rGF/ABS composite (rGF/ABS) at 220 °C.

In order to investigate the printed sample microstructure, and evaluate porosity, fiber orientation/distribution, an x-ray computed chromatography (CT) scan of a printed part was carried out. A cylindrical specimen with a diameter of 6 mm and a length of 30 mm was cut from the printed hexagon from a middle section in the printing direction for the x-ray CT scan. Figure 29 shows the distribution of pores segmented from the low magnification scan for the 3D-printed part. The total pore volume inferred from this scan was calculated as 0.58%. The segmentation quantified the volume of each element. The equivalent pore diameters were calculated from the segmented volumes assuming spherical geometry. The relative frequency was the highest (~29.5%) when the equivalent diameter was 55  $\mu\text{m}$ .

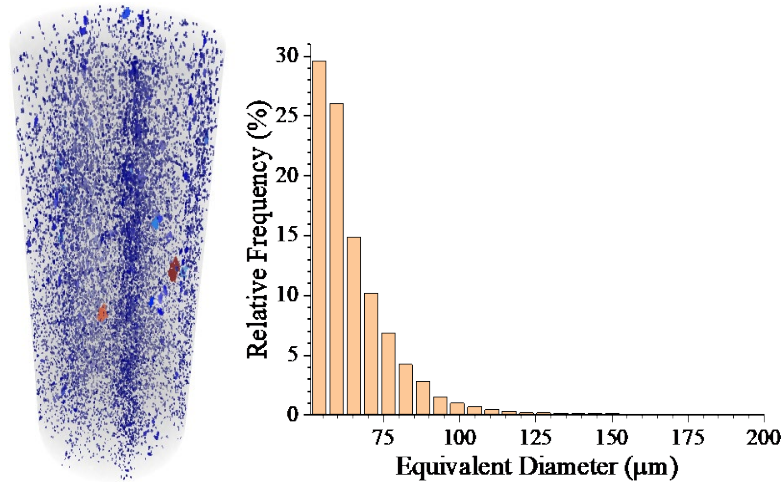


Figure 29. XCT analysis: the distribution of pores segmented from the low magnification scan for the 3D-printed part.

Figure 30 shows the 3D and side images of the scanned area which showed the segmented GFs for the 3D-printed part. The total fiber volume from this scan was calculated as 7.45%. This is also consistent with the value calculated (~7.8%) based on 18 wt% GF (2.7 g/cm<sup>3</sup>) in ABS (1.04 g/cm<sup>3</sup>). Also Figure 30 confirms the tendency of rGFs to align in the printing direction.

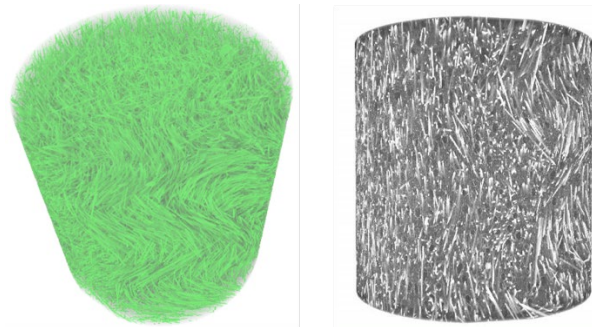


Figure 30. XCT analysis: the 3D images that showed the segmented glass fibers for the 3D-printed part.

Once all the characterization on the printed sample part (i.e., hexagon) was completed, a section of a submersible device was selected as a demo for printing. Since the available material was limited, a relatively small part had to be selected. Also, in order to observe distortion of the material during printing due to residual stress, a two-bead wall curl bar was printed along with the demo part (Figure 31a). The printing parameters that were optimized during hexagon printing were used. While printing the curl bar, some irregularities were observed, but the demo part was printed successfully (Figure 31b and c). One possible explanation for the irregular printing of the curl bar can be the low layer time, and thus poor cooling during printing. Unlike the curl bar, the actual demo part was single bead and could cool faster. Since we only had limited material, another attempt to print the curl bar couldn't be attempted. However, the purpose of the curl bar was to investigate the warpage of the part, and as shown in Figure 31b, only a slight distortion (circled) was observed.

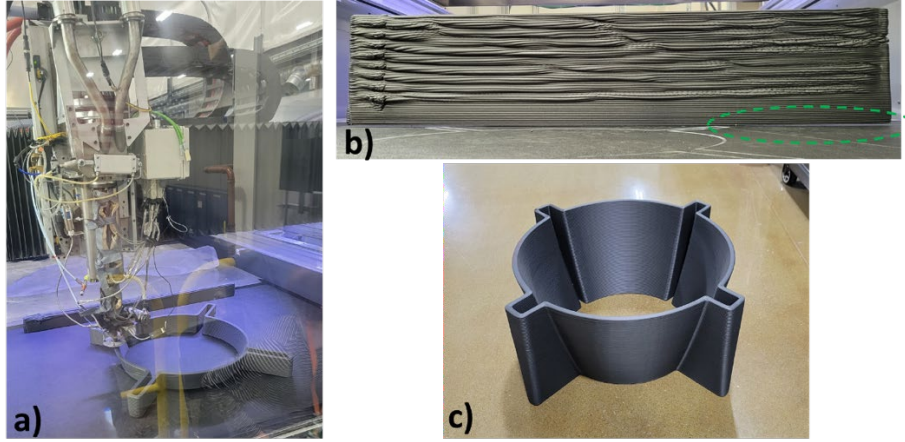


Figure 31. XCT 3D-printed part.

In summary, the rGFs were successfully used to develop a 3D printable composite feedstock material with improved mechanical properties, and it was used to demonstrate printing of a section of a submersible device.

## 6. BENEFITS ASSESSMENT

The focus of the Phase II program was to assess whether cured polymer reinforced composite parts could be processed using the pyrolysis route to efficiently recover the glass and carbon fibers with acceptable properties for sustainable re-use and then to assess the performance of the recovered fibers in the FRP parts.

The Phase II program developed a more optimal processing profile than the profile achieved in the Phase I study with CHZ [1], with a better balance of processing efficiency, gas production and fiber recovery.

### Recovery of Glass Fibers using Pyrolysis

The distribution of embodied energy (EE) of recycled glass fiber is depicted in Figure 32 (left). A lab pyrolysis trial compared the embodied energy of virgin glass fiber to rGF. Both injection molding and bulk molding compound applications were compared to estimate the impact of the recycled composite parts on total EE. As seen in Figure 32 (right), the use of rGF, compared to virgin glass fiber, is estimated to reduce the embodied energy by 27% using injection molding process, while bulk molding compound showed a similar reduction of 22%.

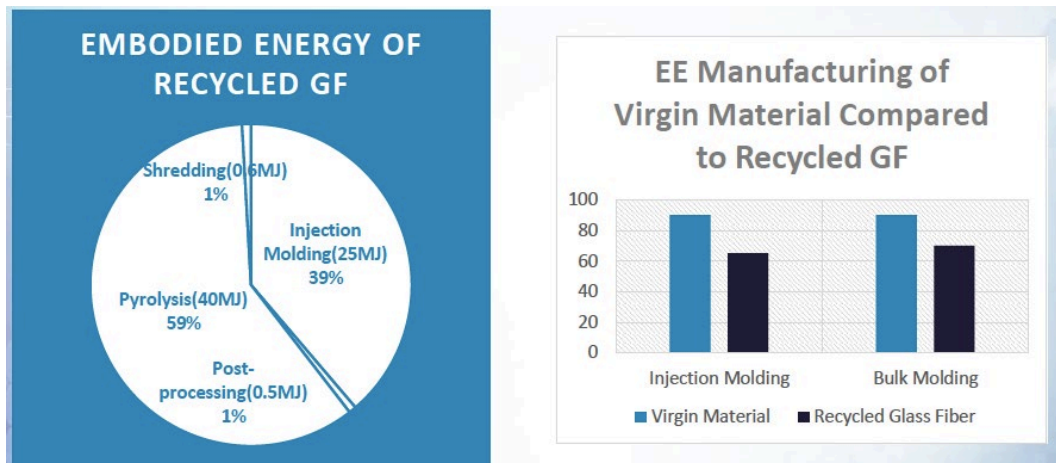


Figure 32. Summary of Embodied Energy (EE) Distribution (left) and Recycled EE Savings (right).

In addition to injection molding and bulk molding processes, 3D printable feedstock material in pellet form with improved mechanical properties was successfully developed using recycled glass fibers, and additive manufacturing of a part was demonstrated.

For pyrolysis of GF, natural gas was used to power the furnace to pyrolyze glass fiber resulting in an embodied energy of 40MJ/kg. Post pyrolysis & transportation: Combing & precision cutting added +0.0001MJ/kg; 200km of nominal transportation was also included which added +0.5MJ/kg

Analytical data from Phase I confirmed that toxic materials in the composites could be safely handled including resins containing halogenated aromatic or aliphatic compounds. Halogenated additives have been used for many years to enhance operation application properties including chemical resistance, fire retardancy, thermal stability, UV tolerance, dimensional stability, and other physical requirements for the widely used composites.

## 7. COMMERCIALIZATION

There are currently two active commercialization activities occurring in part due to Phases I and II of this project.

The Thermolyzer™ pyrolysis process equipment will be produced by Starr Manufacturing, Warren, OH in 10, 22, 44, 88 and eventually 176 ton per day units. The Thermolyzer™ units will be supplied to various companies intending to process EOL materials like tires, electronic plastics & boards, treated wood, plastics & ocean plastics, MSW, and other organic waste materials now including composites. The Thermolyzer™ process will produce a clean renewable Syngas to produce power plus plans to develop a process to recover green hydrogen gas from the Syngas for the hydrogen economy. The solid char produced contains recoverable solid electronic/precious/REE metals, carbon black, Biochar and reinforcing carbon or glass fibers from these composites. These assets lead to an economically defensible process with ROI to support the investment.

First commercial unit has been permitted and site prep started in Youngstown, OH to process tires. Other EOL tire facilities are being designed and permitted to follow the Youngstown, OH based Youngstown Thermal operation.

Testing is in process for electronic scrap plastics and boards (also an epoxy-glass composite), plastics, treated railroad ties/utility poles, Auto Shredder Residue, and community/DOD waste processing. This will lead to plants being built that may have the ability to also process EOL composites in designated campaigns to recover the fibers.

Support for these programs was provided by members of the ACMA, IACMI, ORNL and others familiar with the composite processing work and test confirmation with the recovered fibers. Critical challenge has been with low EOL composite volume, lack of fiber data supporting sustainable re-use and cost challenges of the recovered glass fibers to find processes and economically viable commercial applications.

## 8. ACCOMPLISHMENTS

Different routes of recycled fibers and compounding were demonstrated. In some instances, mixed streams of carbon/glass fibers in conjunction with thermoplastic fibers was successfully processed into intermediates.

Processes including wet layup, twin screw extrusion, extrusion-compression through a plasticator were the approaches demonstrated in developing the intermediates and demonstration products. These approaches are scale able and can be applied to large scale products based on the application need.

The project led to successful demonstrations of representative automotive components: a seat back rest and a battery tray part using recycled intermediates.

Publications are being compiled from the above works. These will take at least 3-4 months past the project period to go through the peer-review process in journals and conferences. We anticipate the work to be presented and published at the Composites and Advanced Materials Expo (CAMX)/Society for the Advancement of Material and Process Engineering (SAMPE), Automotive Composites Conference & Expo (ACCE), and Recycling Conferences. The journals to be targeted will be *Sustainability and Energy*, *Composites Part B* and *Materials Processing Technology*.

An abstract was submitted to the American Society of Mechanical Engineering (ASME), International Mechanical Engineering Congress and Exposition (IMECE) for presenting the results, and a manuscript for a journal article is in preparation. Additionally, two refereed journal publications were generated (both by Zhao, et al., see References).

Two R&D 100 Awards were given in 2018 for the Thermolyzer™ process, including the bronze award for green technology and one of the top 100 most technologically significant new products of the year.

Five Patents have been granted on the Thermolyzer™ process and EOL materials covered by the process. Patent Cooperation Treaty (PCT) filings in the European Union (EU) and Far East are also underway.

Multiple product/material sectors are being reviewed for EOL processing using the Thermolyzer™ process, along with additional confirmation of toxic material destruction of compounds used in those organic polymers including chemicals used for thermal application stabilization, thermal processing stabilization (phthalates), fire retardancy (halogen and phosphorous), application anti-oxidation, UV stability, colorants/pigments, BPA, and other specific polymer properties required by the application.

## 9. CONCLUSIONS

The following conclusions result from the pyrolysis of EOL fiber reinforced polymer composites to recover glass and carbon fibers as well as energy from the resin phase, followed by demonstration part development:

1. The Phase II project recovered fibers with the less thermal and processing stress than Phase I.
2. In addition, more complete gasification of the composite polymer from process conditions resulted in a process that provides more of the energy required from the resin, foam, and wood fiber contained in the recyclate.
3. Wind blades are difficult to shred and thermally process due to the size and construction.
4. The Thermolyzer<sup>TM</sup> process was successfully modified to process GF from the wind turbine blade shreds. The reactor modifications in Phase II together with process optimization resulted in successful recovery of the glass fibers sufficient to evaluate their use in FRP composite demonstration products.
5. Properties of the recovered recycled fibers from the ideal process conditions would be considered typical of commercial composite processes with the Thermolyzer<sup>TM</sup> technology. It is anticipated that these processing conditions could be scaled up for larger scale or commercial scale production.
6. Mixed streams have a higher BTU content, which results in more syngas production. This in turn supports more complete combustion during pyrolysis and improves fiber recovery efficiency.
7. Handling recovered carbon fiber and transforming into useful products is a challenge; several methods in this program have shown ways of enabling the fiber handling.
8. Twin screw compounding results in fiber attrition which can be detrimental to the resulting composite properties.
9. Wet lay is a viable process to retain fiber length and generated recycled glass fiber intermediates.
10. Prototype aluminum tools were adequate for proof of concept and materials evaluation work to demonstrate production of parts/test articles.
11. Recycled fibers can be successfully converted into composites via various approaches including BMC, wet lay, extrusion-compression, additive manufacturing, and related processes.
12. There is loss of strength in the recycled glass fibers and carbon fibers. However, the strength was sufficient for up to 20% substitution of recycled fibers using certain composite processes, such as bulk molding compound.
13. Hybrid glass/carbon intermediates can be explored in the future projects to obtain the balance of stiffness and impact resistance.

## 10. RECOMMENDATIONS

Phases I and II of project have demonstrated that it is feasible to recover glass and carbon fibers from fiber reinforced polymer composites, including end-of-life materials such as wind blades, automotive/truck parts, and agricultural parts. This project has helped to catalyze the commercialization of the pyrolysis process to recover energy and fibers from end-of life and scrap composite materials. Additional demonstration projects would help to increase market pull for recycled composite materials.

The pyrolysis process could be seen as part of a larger circular economy supply chain for composite materials. The circular economy supply chain already includes grinding and cement kiln processing. Additional work to support the development toward reuse and remanufacturing of end-of-life composite materials is recommended to capture even more of the intrinsic value of the composite material to improve the overall life cycle impact of composite products.

## 11. REFERENCES

- [1] Coughlin, Daniel, Ludwig, Charles, Ozcan, Soydan, Hartman, Dave, and Ginder, Ryan. *Controlled Pyrolysis: A Robust Scalable Composite Recycling Technology*. United States: N. p., 2021. Web. doi:10.2172/1762486.
- [2] Technology Roadmap, IACMI-The Composites Institute, [www.iacmi.org](http://www.iacmi.org), June 2017.
- [3] Recycling technologies, Mini-Road Map, IACMI-The Composites Institute, [www.iacmi.org](http://www.iacmi.org), June 2018.
- [4] Ginder, R. & Ozcan, S. (2019). Recycling of Commercial E-glass Reinforced Thermoset Composites via Two Temperature Step Pyrolysis to Improve Recovered Fiber Tensile Strength and Failure Strain. *Recycling*, 4(2). doi:10.3390/recycling4020024.
- [5] Ginder, R., Ker, D., & Ozcan, S. (2019). Degradation of E-glass fiber mechanical properties during composite sheet molding compound production for automotive applications. *MRS Communications*, 9(4), 1256-1260. doi:10.1557/mrc.2019.145.
- [6] A.T. Brady, B. D. Mannhalter and D.R. Salem, "Discontinuous-fiber composites and methods of making the same", US Patent 10,920,041 (2021).
- [7] D.R. Salem, New Life for Recycled Fibers in Laminated Thermoplastic Composites, *Composites Manufacturing*, May 3, 2019
- [8] Zhao, X., Li, K., Wang, Y., Tekinalp, H., Larsen, G., Rasmussen, D., Ginder, R.S., Wang, L., Gardner, D.J., Tajvidi, M., Webb, E., and Ozcan, S. High-Strength Polylactic Acid (PLA) Biocomposites Reinforced by Epoxy-Modified Pine Fibers. *ACS Sustainable Chemistry & Engineering*. 8 (35): 13236-13247, 2020.
- [9] Zhao, Xianhui, Halil Tekinalp, Xianzhi Meng, Darby Ker, Bowie Benson, Yunqiao Pu, Arthur J. Ragauskas et al. "Poplar as biofiber reinforcement in composites for large-scale 3D printing." *ACS Applied BioMaterials* 2, no. 10 (2019): 4557-4570.
- [10] <https://www.recyclingtoday.com/article/eref-releases-analysis-national-msw-landfill-tipping-fees/>
- [11] <https://www.topmarkfunding.com/freight-rates-mostly-unchanged-for-august-2021/>
- [12] [https://ops.fhwa.dot.gov/freight/policy/rpt\\_congress/truck\\_sw\\_laws/app\\_a.htm](https://ops.fhwa.dot.gov/freight/policy/rpt_congress/truck_sw_laws/app_a.htm)